Coordinated Predictive Control of a Hydropower Cascade

Andrew Hamann
Advisor: Prof. Gabriela Hug

Carnegie Mellon University
Department of Engineering and Public Policy

Pittsburgh, Pennsylvania
March 2015

Acknowledgements

This report summarizes the research that I conducted with the Hydro Research Foundation as a recipient of the Hydro Fellowship. I was awarded the Hydro Fellowship in April 2013, and conducted research with the financial support of the Hydro Research Foundation from June 2013 to December 2014. The Hydro Research Foundation also provided invaluable logistical support for my research, including connecting me with the utilities and companies that wound up advising my research and could benefit from it in the future. I am grateful to the Hydro Research Foundation for their support of my work, and I thank Brenna and Deborah for assisting my graduate school studies.

This research was also funded by the Electric Power Research Institute; the Robert W. Dunlap Graduate Fellowship, awarded by the Steinbrenner Institute for Environmental Education and Research at Carnegie Mellon University; the Bertucci Graduate Fellowship, awarded by Carnegie Mellon University; and the Department of Engineering and Public Policy at Carnegie Mellon University.

Executive Summary

Hydropower is an important renewable energy resource. It is low-carbon, emits nearly no particulate pollution, can ramp quickly, and is capable of storing energy across many hours or days. While it is a very valuable resource by itself, hydropower can also serve as a key enabler for the increased penetration of non-dispatchable renewable energy resources like wind and solar power.

This project focused on developing an optimization-based coordinated control framework for a hydropower cascade. It consisted largely of two parts. The first is the development of the coordination scheme. The second is the simulation and state estimation tools that were developed to allow comparisons between historical operations and the operations dictated by the coordination scheme.

The coordinated control scheme that we developed is based on a control technique known as Model Predictive Control (MPC), wherein a linear state space model is designed to model the hydraulics of a hydropower cascade. Here, the hydraulics model describes how water flows in a hydropower cascade change the reservoir elevations behind each hydropower plant. The model accounts for the delay between water discharged from the upstream plant affecting the forebay elevation of the downstream plant.

The control scheme also accounts for the non-linear character of tailrace elevations. There is an obvious relationship between the amount of water discharged into the tailrace and the tailrace elevation. Our modeling work takes that a step further by identifying the conditions that lead to encroachment and modeling encroachment. Encroachment is when the downstream forebay backs up into the upstream tailrace, causing the tailrace elevation to be higher than it would be otherwise.

The optimization scheme also accounts for the relationship between turbine discharge, hydraulic head, and powerhouse generation in a hydropower plant. Turbine discharge and hydraulic head are mapped to a corresponding amount of powerhouse generation using a three-dimensional piecewise planar function. This function is fit to historical operations data. Since the relationship between the three variables can be represented using a set of linear functions, the model for hydropower production can be integrated into a linear or quadratic program. This results in an optimization model that is both fast and accurate, an improvement over other coordinated control schemes that are based on nonlinear or mixed-integer programming.

The objective function was formulated to minimize the sum of the squared turbine discharge and spill for each hydropower plant. The weights were chosen such that water was preferentially discharged from large surface area reservoirs to small surface area reservoirs. This allocates a certain volume of water such that it results in the maximum total hydraulic head. Weighting turbine discharges in this way is unique in the hydropower optimization literature.

We tested the coordinated control scheme on the Mid-Columbia hydropower system. The Mid-Columbia consists of seven dams on the Columbia River in Eastern Washington State. Historical data on system operations allowed us to benchmark the performance of our coordination scheme with actual system operations. Further data was provided that allowed us to properly calibrate the

parameters of our model, including forebay and tailrace curves, travel times, and hydropower production functions.

Simulations were conducted for a five-day period with five-minute time resolution. The results of our simulations, in brief, can be condensed into four areas.

1. The hydraulic potential of the system (H/K) increased steadily over the course of the simulations. At the end of the simulation period, the total system H/K was 0.6% higher than in the historical case. This translates to several feet of additional hydraulic head.

2. The net energy stored in the cascade increased. Overall, the net energy benefit was 1708 MWh, or 0.33% of the total energy generated during the simulation period. In general, Grand Coulee ran an energy deficit (i.e., its forebay was lower in the optimized case than the historical case) and the remaining hydropower plants ran an energy surplus.

3. Ramping was reduced substantially. Quantitative measures indicated that ramping decreased substantially at every hydropower plant besides Grand Coulee. Qualitatively, the discharge profiles were much smoother in the optimized case than in the historical case. This method of operation could have substantial (but uncertain) benefits to hydropower plant owners and operators due to less unit cycling and ramping, which results in lower maintenance and repair costs.

4. System constraints were satisfied. The Mid-Columbia system is constrained at many times of the year due to environmental limits on turbine discharge, spill, and flow ramping. These limits are designed to ensure the health of salmon runs on the Columbia River and the spawning areas in the Hanford Reach downstream of Priest Rapids. One of the primary benefits of doing coordinated control in an optimization framework is that system constraints can be explicitly obeyed. This ensures that regulatory and legal bounds on system operations are satisfied completely.

The second part of the research involved the development of a state estimation procedure for a hydropower cascade. Evaluating the coordinated control scheme necessitated developing a state estimation procedure to reconcile measured values of turbine discharge, spill, and forebay elevation. In lieu of being able to test the outputs of the coordinated control scheme on the actual Mid-Columbia system or on a high-fidelity simulator, an inherently inaccurate computer model must be used. This model will contain some modeling errors. Likewise, the measured flows and forebay elevations can be biased and noisy.

These biases and noise levels are unknown and, *a priori*, we do not know which values can be trusted and to what extent. The state estimation procedure takes these values and the hydraulic model, and adjusts the measurements such that the model is open-loop stable and the estimated measurements are consistent with each other. The general idea is that one flow measurement is assumed to be the true flow through the system, and the other flows (upstream and/or downstream) are adjusted to reduce the residual error between the estimated flow and the measured flow. Constraints are added to the procedure to ensure that the estimated flow profile is similar to the measured flow profile. Results are given demonstrating the practical efficacy of the proposed state estimation method.

Contents

List of Figures

List of Tables

1 Introduction

Hydropower is an important energy resource in many parts of the United States, most especially in the Pacific Northwest region. It is the primary source of renewable electricity generation in the United States and the world, and it possesses unique characteristics that make it useful to electric power system operators. Hydropower needs less time than coal- or gas-fired power plants to ramp its generation basepoint. Reservoirs and hydropower systems with large storage capacities also have the ability to arbitrage energy generation across hourly or daily time frames; this is done by deferring hydropower production when other electricity generation is cheap, and generating more electricity when other generation is more expensive or less efficient. Additionally, once hydropower is built, it is emits low levels of particulates and carbon dioxide.

Currently, the electric power system is transitioning from a system based on thermal and hydro generation to one that incorporates substantial amounts of wind and solar power. Wind and solar resources are intermittent (i.e., the wind does not always blow and the sun does not always shine) and variable (i.e., we cannot predict with perfect accuracy when and how much wind will blow or sun will shine). This presents a number of challenges to system operators. The ability to arbitrage energy and ramp quickly means that hydropower is uniquely positioned to address intermittency and variability from renewable energy resources. As the electric power system continues its transition to a low-carbon future, the role of hydropower, especially in the Pacific Northwest, stands to increase in importance.

This project is concerned with developing a coordinated control scheme for a hydropower cascade. In this research, the term *cascade* refers to two or more hydropower plants situated along the same river or in the same river system. These hydropower plants are hydraulically coupled such that the flows from one hydropower plant affect the reservoir of the downstream hydropower plant. Hence, the flows from each hydropower plant should be coordinated to avoid unnecessary spill, maintain stable reservoir elevations and flows, and keep hydraulic heads as high as possible. Coordinated control schemes can vary in complexity, but the central tenet behind coordinated control is that operating the system as a whole can increase the efficiency of the system well beyond that which could be achieved by operating the system as discrete, unconnected hydropower plants.

Section 2 details the coordinated control scheme that we developed for the Mid-Columbia hydropower system. The Mid-Columbia system consists of seven dams located on the Columbia River in the United States. The state space model accounts for system hydraulics, including water travel times and dynamic tailrace elevations. We accurately approximate the power generation from a hydropower plant using a piecewise planar function of turbine discharge and hydraulic head. We demonstrate how this approximation can be written as a set of linear constraints and integrated into a quadratic program. We introduce an objective function that maximizes efficiency by maximizing hydraulic head. Compared to historical operations, the proposed control scheme reduces ramping, increases total system hydraulic head, increases the energy content in the system at the end of the simulation period, and operates the system within all elevation and flow constraints.

Section 3 describes a state estimation method for estimating discharges from hydropower plants. The optimization, control, and simulation of cascaded hydropower systems requires a

computational model for system hydraulics. Since this model is an approximation of some physical reality, it will inevitably contain inaccuracies. When doing an open-loop simulation using the developed system model and historical measurements of the system (e.g., discharge and forebay elevation), these small modeling errors will accumulate and propagate, resulting in errors that increase with the length of the simulation. Measurement noise and bias only exacerbates the problem. However, determining the worth of a proposed control scheme necessitates comparing it to a historical baseline. Without accounting for measurement error, which is typically unknown or uncertain, directly comparing historical discharges to those computed by the control scheme would be like comparing apples to pears.

In Section 3, we propose a method that uses a hydraulic model, historical data, and state estimation to compute estimated discharges and forebay elevations, thus allowing a true apples to apples comparison. State estimation is a mathematical technique that can be used to reconcile the discharge measurements with the recorded forebay elevations. Since forebay elevation measurements are more accurate than flow measurements, they are assumed to reflect the "true" system state. The inputs to the method are the historical discharge and forebay elevation measurements, and the outputs are the estimated discharges and forebay elevations. Using these values, it is then possible to compare a simulated control scheme with the historical operations of the system in a reasonable and accurate way. Example simulations are done using data from the Mid-Columbia hydropower system.

2 Real-Time Optimization of the Mid-Columbia Hydropower System

Introduction

The operation of cascaded hydropower plants (HPPs) as an integrated system is known as coordinated control. Coordinated control improves the ability of each HPP to meet its regulatory and environmental limits on turbine discharge, spill, and forebay elevation. Coordination provides other ancillary benefits, including the reduction of turbine-generator ramping and cycling, maintenance of stable forebay elevations, provision of additional scheduling flexibility for HPP stakeholders, and efficient water use.

Since every hydropower facility and system is unique, coordinated control schemes are tailored to particular systems, regions, and operating objectives. As a result, they can have significantly varying capabilities and complexity. Approaches include those based on heuristics [1], genetic algorithms [2], mixed-integer linear programming [3-5], nonlinear programming [6], and dynamic programming [7]. Determining what variables are important and how those variables should be modeled and optimized is a design decision that varies according to the scope of the proposed control scheme.

This section presents a real-time control scheme for the Mid-Columbia hydropower system. The Mid-Columbia system consists of seven dams along the Columbia River. Our research objective is to analyze the performance improvements of doing optimization in real-time operations, relative to the historical dispatch of the Mid-Columbia system.

We were provided two sets of data for the Mid-Columbia system. Each set of data contains time stamped measurements of turbine discharge, spill, forebay elevation, tailrace elevation, power generation, and the anonymized generation requests of individual stakeholders. The data sets also include real-time minimum and maximum limits for forebay elevation, turbine discharge, and generator ramping. The first set of data was provided at five-minute resolution for all of 2012 (105,408 sample points). The second set of data was provided at one-minute resolution for six representative weeks in 2013 (60,480 sample points). These data sets will be referred to as the five-minute dataset and one-minute dataset, respectively.

The section is organized as follows. “Hydraulic Model” describes the state space model of the hydropower cascade. “Hydropower Production Function” introduces the piecewise planar approximation of the hydropower production function and how we incorporate it as a set of linear constraints. “Optimization Problem” reviews the optimization problem and the formulation of the objective function. “Case study” presents a case study evaluating our proposed control scheme against the historical operation of the Mid-Columbia system. “Conclusion” concludes this section.

Hydraulic Model

The proposed control scheme employs Model Predictive Control (MPC), a type of receding horizon control in which a linear state space model is used to predict the reaction of a system to a set of control inputs. The designer creates an objective function that maps the future values of the control inputs, system state, and system outputs to a scalar evaluation metric. Using linear or

quadratic programming, the control sequence that delivers the best performance over the time horizon is computed. The first step of this control trajectory is then applied, and the system is observed at the next time step. This procedure repeats indefinitely. Linear, time-discrete MPC models have the general form

$$\mathbf{x}(k+1) = A\mathbf{x}(k) + B\mathbf{u}(k) \quad \text{for } k = 0,\ldots,K-1 \tag{2.1}$$

$$\mathbf{y}(k) = C\mathbf{x}(k) \quad \text{for } k = 1,\ldots,K \tag{2.2}$$

Where $\mathbf{u}(k)$ is the vector of control variables, $\mathbf{x}(k)$ is the vector of state variables, and $\mathbf{y}(k)$ is the vector of observed variables. The A and B matrices describe the relationship between the control inputs, current system state, and future system state. Similarly, the C matrix is the relationship between the system state $\mathbf{x}(k)$ and the observed system state $\mathbf{y}(k)$. K is the discrete time-horizon over which the system is optimized. Constraints on state, control, and observed variables are explicitly incorporated into the MPC model. Additionally, since the state variable cannot change instantaneously, $\mathbf{x}(0)$ is a fixed value reflecting the initial system state.

Hydraulic coupling of sequential reservoirs

In a cascaded hydropower system, hydraulic coupling can be modeled with a water balance equation in which water discharged from the upstream HPP arrives in the reservoir of the downstream dam after some travel time. (Since the Mid-Columbia system does not have any branching, our hydraulic modeling assumes that the cascaded system is situated on a single river. However, these equations can be generalized to cascaded systems containing two or more rivers [8].) Mathematically,

$$x_j(k+1) = x_j(k) - \frac{t_k}{\Psi_j}\left(q_j(k) + s_j(k)\right) + \frac{t_k}{\Psi_j}\left(w_j(k-\tau_j) + q_{j-1}(k-\tau_j) + s_{j-1}(k-\tau_j)\right) \tag{2.3}$$

Where the natural inflow into the reservoir behind dam j is denoted by $\mathrm{w}_j(\mathrm{k})$; turbine discharge and spill through dam j is denoted by $q_j(k)$ and $s_j(k)$, respectively; and the water level behind dam j is denoted by $x_j(k)$. There are a total of J dams in the cascade. Ψ_j is the effective surface area of the reservoir behind dam j. The model is discretized by t_k, the length of the optimization interval. The t_k/Ψ_j term in (2.3) maps water flow into or out of reservoir j to a proportional increase or decrease in the elevation of reservoir j. The travel time τ_j between dam $j-1$ and dam j is normalized by the optimization time step t_k. In our previous work, we implicitly set $\tau_j = 0$ [9]. In this research, we were provided travel times for each reach in the Mid-Columbia system, information that we used to improve the model.

The state space model used in MPC relates the system state and control inputs at time k with the system state at the next time step $k+1$. Since the travel time between each dam is several times the length of the optimization time step, the formulation in (2.3) cannot be used directly in the state space model. Thus, we introduce additional state variables, denoted by $b_{j,m}(k)$. In physical

terms, $b_{j,m}(k)$ can be interpreted as the volume of water discharged from dam $j-1$ during time step $k-m$.

For each dam j, there are M_j of these variables, where

$$M_j = \lceil \tau_j \rceil. \tag{2.4}$$

From the use of the ceiling operator $\lceil \square \rceil$ in (2.4), and the fact that the time delay $\tau_j > 0$, it is obvious that $M_j \in \mathbb{Z}^+$ for $j = 1,\ldots,J$. (For the first dam in the cascade, the travel time τ_1 is dependent on the location of the inflow gauge.)

We can now rewrite (2.3) as a series of three relationships that couple the discharge from dam $j-1$; the volume of water in $b_{j,m}$ for all $m = 2,\ldots,M_j$; and the forebay elevation x_j. The state delay variables are specified as

$$b_{j,1}(k+1) = t_k\left(w_j(k) + q_{j-1}(k) + s_{j-1}(k)\right) \tag{2.5}$$

$$b_{j,m}(k+1) = b_{j,m-1}(k) \tag{2.6}$$

and the forebay elevation is specified as

$$x_j(k+1) = x_j(k) + \frac{1}{\Psi_j} b_{j,M_j}(k) - \frac{t_k}{\Psi_j}\left(q_j(k) + s_j(k)\right). \tag{2.7}$$

Next, we introduce limits on the state and control variables corresponding to each dam j

$$q_j^{\min} \le q_j(k) \le q_j^{\max} \tag{2.8}$$

$$s_j^{\min} \le s_j(k) \le s_j^{\max} \tag{2.9}$$

$$w_j^{\text{pred}}(k) \le w_j(k) \le w_j^{\text{pred}}(k) \tag{2.10}$$

$$x_j^{\min} \le x_j(k) \le x_j^{\max} \tag{2.11}$$

where (2.8) and (2.9) limit turbine discharge and spill to fixed minimum and maximum values and (2.10) limits natural inflow to values determined by a forecast. Limits on forebay elevation (2.11) are dictated by the regulatory, environmental, and operational constraints specific to each catchment. We consider limits on state and control variables to be static for the time horizon of interest, but the modeling approach could incorporate constraints that vary with time.

Modeling tailrace elevation

The tailrace is the water immediately downstream of a dam into which the spillway and turbines discharge. The tailrace elevation directly affects the hydraulic head, which in turn affects the power generated in the turbines. Hence, accurately modeling power generation necessitates accurately modeling the tailrace elevation. There is a direct and substantial relationship between

the water discharged into the tailrace and the water level in the tailrace. In the literature, non-linear optimization techniques typically model this relationship using polynomial functions of turbine discharge [10-12]. Linear or quadratic programming models often use an affine tailrace function [13].

In our previous research [9], the tailrace elevation above sea level z_j was computed as

$$z_j(k+1) = \alpha_j \cdot q_j(k) + z_j^0 \tag{2.12}$$

where α_j and z_j^0 were parameters fitted using ordinary least-squares regression. Further analysis of the tailrace measurement data indicated that the tailrace elevation was also correlated with the downstream forebay elevation. Adding a term for the forebay elevation, we modified (2.12) to be

$$z_j(k+1) = \alpha_j \cdot q_j(k) + \gamma_j \cdot x_{j+1}(k) + z_j^0 \tag{2.13}$$

where α_j, γ_j, and z_j^0 were parameters fitted using ordinary least-squares regression. This improved the performance of the tailrace function markedly. However, there were still instances where the predicted tailrace elevation was many tens of centimeters lower or higher than the actual tailrace elevation. This occurs because the tailrace elevation can have a non-continuous dependence on the downstream forebay elevation, moving between two modes: encroached and not encroached. Encroachment in the Mid-Columbia system is a problem that has been identified and is accounted for by system operators.

Here, we introduce the variable ϕ_j to represent the encroachment status of dam j. When dam j is encroached, $\phi_j = 0$. When dam j is not encroached, $\phi_j = 1$. When the tailrace is transitioning between the two modes (i.e., $0 < \phi_j < 1$), dam j is said to be partially encroached. Whether or not a dam is encroached depends on the tailrace elevation of the upstream HPP and the downstream forebay elevation. If the upstream tailrace elevation is high due to increased discharges and the downstream forebay has been drafted, the dam will not be encroached. Similarly, if the upstream discharges are low and the downstream forebay is near its maximum elevation, the upstream dam will likely be encroached. So, we define ϕ_j as a function of $\delta_j(0)$, where

$$\delta_j(0) = z_j(0) - x_{j+1}(0). \tag{2.14}$$

We elected to define ϕ_j as a piecewise linear approximation to the logit function, shown in Figure 2-1, although any classification function that is both monotonically non-decreasing and constrained to be between 0 and 1 could be used.

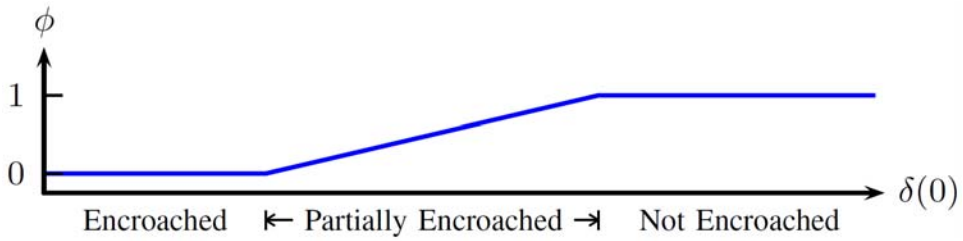

Figure 2-1
General form of the encroachment classification function φ

A new value for ϕ_j is computed before each optimization interval using the system state variables at $k = 0$ (i.e., the definition of δ_j in (2.14)). We then redefine the tailrace function (2.13) to be

$$z_j(k+1) = \phi_j \cdot z_j^1(k+1) + (1-\phi_j) \cdot z_j^2(k+1) \tag{2.15}$$

where

$$z_j^1(k+1) = \alpha_j^1 \cdot q_j(k) + \gamma_j^1 \cdot x_{j+1}(k) + z_j^{0,1} \tag{2.16}$$

$$z_j^2(k+1) = \alpha_j^2 \cdot q_j(k) + \gamma_j^2 \cdot x_{j+1}(k) + z_j^{0,2} \tag{2.17}$$

in which we fit two sets of regression parameters, partitioning the data according to the classification function ϕ_j. The slope and intercept parameters for ϕ_j were selected via an exhaustive search for the ϕ_j that resulted in the smallest mean squared error. Note that using (2.15) instead of (2.13) does not affect the complexity of the MPC model, because ϕ_j is determined before each MPC optimization run. In other words, (2.15) will be simplified to an equation that looks like (2.13) before each run of the MPC optimization model. Note also that the model proposed in (2.15) contains the affine term z_j^0, so we compute the linear term using the state space model and then add the affine term whenever we need to compute the tailrace elevation in meters above sea level [9]. This is necessary in order to compute hydraulic head h, which is the difference between the forebay and tailrace elevations, or

$$h_j(k) = x_j(k) - z_j(k). \tag{2.18}$$

Table 2-1
Performance evaluation of different tailrace models

		Standard Error (m)			Error (p.u.)	
j	Name	1	2	3	2	3
1	Grand Coulee	0.219	0.155	0.127	0.718	0.612
2	Chief Joseph	0.288	0.169	0.101	0.580	0.350
3	Wells	0.152	0.151	0.119	1.026	0.792
4	Rocky Reach	0.134	0.135	0.105	1.008	0.786
5	Rock Island	0.423	0.291	0.287	0.723	0.685
6	Wanapum	0.183	0.133	0.110	0.707	0.581
7	Priest Rapids	0.373	–	–	–	–

To make the case for why the tailrace model in (2.15) is necessary, we collected statistics on the performance of the models described by (2.12), (2.13), and (2.15), denoted as Model 1, 2, and 3, respectively. The tailrace elevations predicted using Model 3 were calculated using the value for ϕ_j computed one hour prior. These results are shown in Table 2-1. Data was trained on the one-minute dataset and tested on the five-minute dataset. The first three columns of data contain the standard error for the testing sequence. The final two columns show the standard error for Models 2 and 3 normalized by the standard error obtained using Model 1. This table illustrates a marked improvement when using Model 3 for several of the projects in the cascade, especially Grand Coulee, Chief Joseph, and Wanapum. Figure 2-2 shows the predicted and modeled tailraces for Chief Joseph Dam. From the figure, we again note the substantial performance gain and increase in predictive power obtained using Model 3.

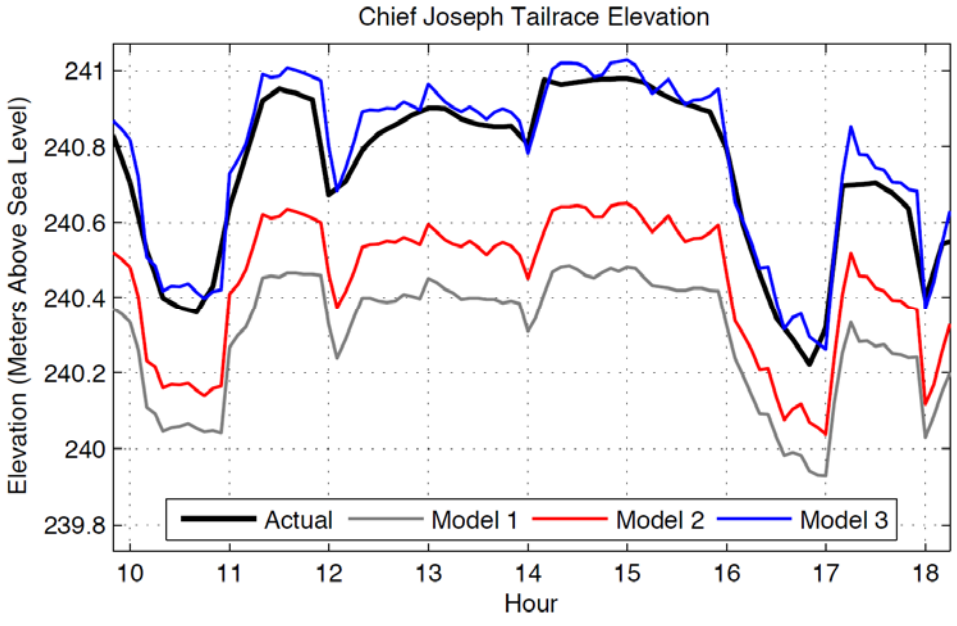

Figure 2-2
Graphical comparison of different tailrace models

Hydropower Production Function

Nonlinear hydropower production function

The amount of gross electrical power extracted from a hydro turbine-generator is a non-linear function of turbine efficiency η_t, generator efficiency η_g, turbine discharge q, and hydraulic head h [14]. This is known as the hydropower production function (HPF). Mathematically,

$$p(\eta_t, \eta_g, q, h) = \kappa \cdot \eta_t \cdot \eta_g \cdot q \cdot h \tag{2.19}$$

where p is the gross electrical power produced by the generator and κ is a conversion constant. We can rewrite (2.19) to be

$$p(q, h) = \kappa \cdot \eta_t(q, h) \cdot \eta_g(q, h) \cdot q \cdot h \tag{2.20}$$

if we assume that turbine and generator efficiencies are functions of hydraulic head and discharge. Generator efficiency is typically greater than 95% and is monotonically non-decreasing with increased generator loading [15]. The efficiency curve for an individual turbine is a concave function commonly referred to as the hill chart. Turbine efficiency can be as low as 60% at minimum discharge and as high as 95% at the best efficiency point [15]. The shape of the hill chart varies depending on the design and age of the turbine [16]. The HPF (2.20) can also contain additional terms, such as losses associated with the friction of water in the penstocks or trash racks. These terms can either be considered explicitly or modeled as a reduction of the net hydraulic head [11],[14].

The detail with which the HPF needs to be incorporated into an optimization or planning model depends on the time horizon, temporal resolution, scale, and goals of the model. For example, head and efficiency effects in long-term optimization can be ignored because powerhouses can be reasonably expected to operate near some average efficiency and hydraulic head. In short-term optimization, as discussed in this research, modeling should be done with a fine enough temporal resolution that captures the rapidly changing system state. Hence, the HPF must be fully modeled as a function of the turbine discharge q and the hydraulic head h. Explicitly considering the efficiency terms and the bilinear qh term requires approaches rooted in non-linear or mixed-integer programming [5],[6]. Unfortunately, these models have a high computational cost and suffer from the curse of dimensionality, limiting their applicability to cascaded systems or to optimization across long time horizons. Reducing computational complexity and decreasing run times generally requires assuming that hydraulic head is constant and the HPF is concave. This can be achieved by approximating the HPF with a set of piecewise linear constraints [3],[8].

In the literature, most hydro scheduling models fall into one of two categories: accurate and slow, or inaccurate and fast. However, the problem of real-time coordination of cascaded hydropower plants requires an optimization approach that is both computationally efficient and accurate. The optimization must be efficient since it should be able to run in real-time. (From a practical standpoint, studies that simulate real-time optimization would not be feasible if each optimization time step took too long.) The optimization approach must also be accurate across a range of operating parameters in order to account for quickly changing system conditions. The primary contribution of this part of our work lies in how we linearize the HPF and integrate it

into an MPC optimization framework. Here, we extend and revise the methods contained in our previous paper [9].

Our optimization model does not account for the scheduling and dispatch of individual turbine-generator units. Rather, we optimize each HPP at the powerhouse level [17]. The reason for doing this is threefold. First, it is difficult to find data that can fully and accurately characterize the efficiency curves and various loss functions in an HPP [14]. Hill charts, when they are available, can be many years or decades old. Second, optimizing the cascade at the unit level would increase the computational complexity, scale, and solution time of each optimization problem. Third, and most importantly, coordination on the Mid-Columbia system does not reach into the powerhouse of individual HPPs. The system coordinator sets the generation basepoint for each HPP but does not specify how many units should be online or what their dispatches should be. As such, there is little utility in modeling a part of the Mid-Columbia system that is neither controllable nor observable by the system coordinator.

Linearizing the hydropower production function

In order to create an accurate model, we need to approximate the HPF using a function of turbine discharge and hydraulic head without explicitly considering the terms on the right-hand side of (2.20). In order to create a fast model, we need to be able to write that approximation as a set of linear constraints without employing mixed-integer variables [5],[18],[19]. Since using a simple three-dimensional linear function was not sufficient, we elected to employ a piecewise planar approximation of each HPF.

Our linearization process is a standard segmented regression with continuity and convexity constraints [20]. In a segmented regression, the covariates are partitioned into sections and a separate linear function is fit to each section. Since the number and position of each section is pre-selected, the problem is computationally simple. In our regression, the covariates are the turbine discharge q, hydraulic head h, and an intercept term. Each partition is defined as the triangle formed by a triplet of (q,h) coordinates. The problem simplifies to a constrained least-squares quadratic program with dimension proportional to the number of partitions.

The regression is fit to data from the one- and five-minute datasets. The partitions are selected in an *ad hoc* fashion, since selecting the optimal number and position of the partitions is a computationally intractable problem. The partitions have the constraint that $h \in \left\{h^{\max}, h^{\min}\right\}$ and $q^{\min} \le q \le q^{\max}$. The maximum and minimum hydraulic heads are selected such that the approximated HPF covers the feasible set of q and h. Additionally, we add a constraint so that the function is concave in the $\hat{q}$ direction for all values of h. Figure 2-3 shows the approximated HPF for Wells Dam and the sample points used in the regression.

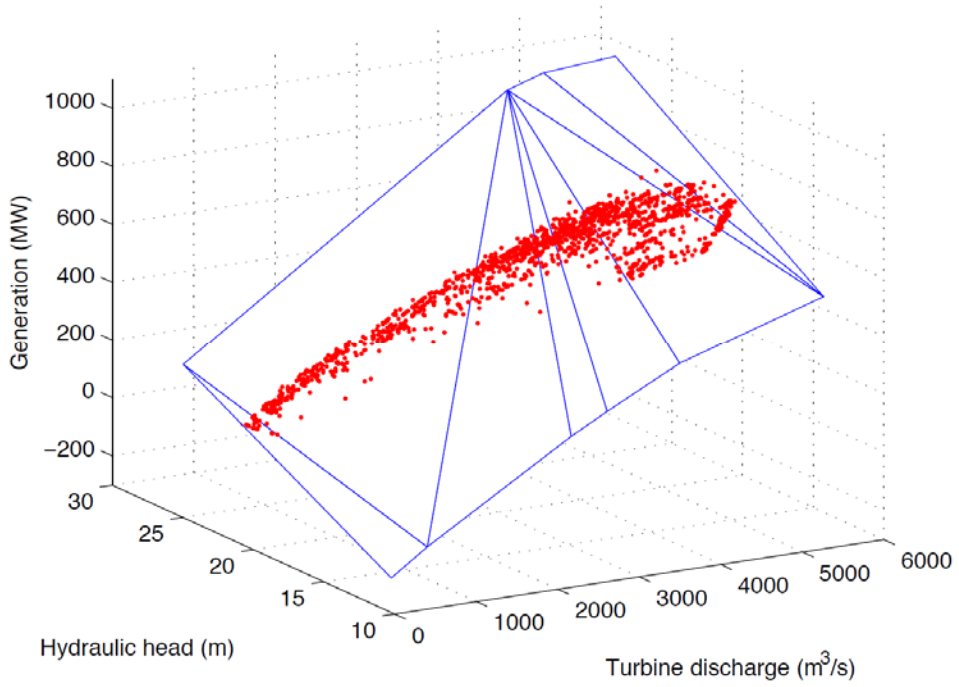

Figure 2-3
Approximated hydropower production function for Wells Dam

Auxiliary variables for discharge and generation

For each section of the piecewise linear approximation of the hydropower production function, we introduce auxiliary variables q_j^i and p_j^i that correspond to the turbine discharge and power associated with each section of dam j. No separate variables are needed for hydraulic head. These three variables create equality constraints for each section i of the piecewise linear function of the form

$$p_j^i(k) = \beta_j^{0,i} + \beta_j^{h,i} \cdot h_j(k) + \beta_j^{q,i} \cdot q_j^i(k) \tag{2.21}$$

where the β's are computed in the fitting process and I_j is the number of sections in the HPF approximation for dam j. Figure 2-4 demonstrates how these variables are assigned.

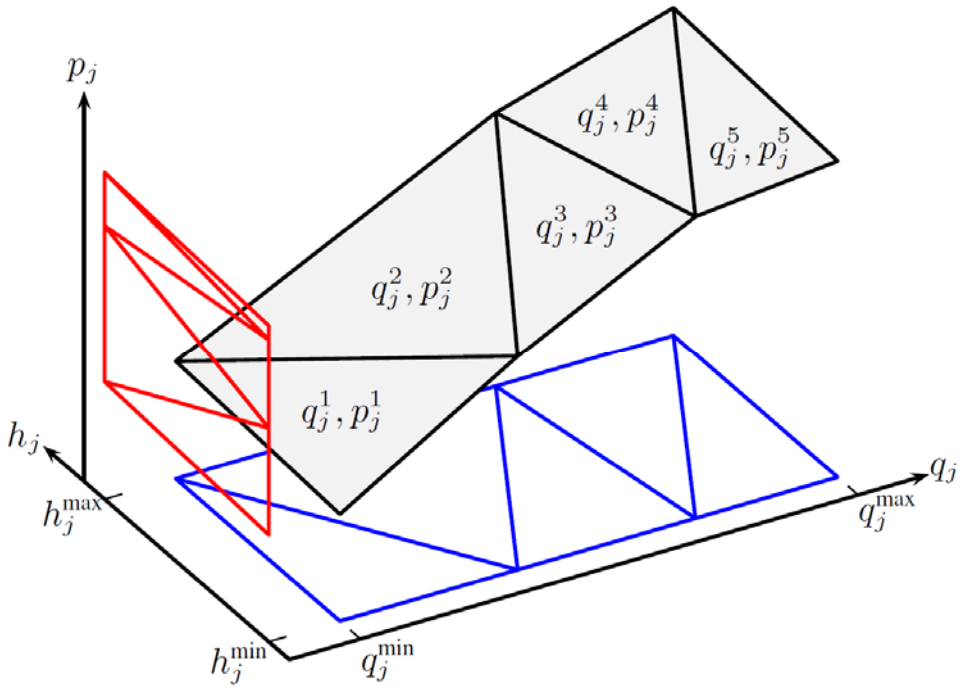

Figure 2-4
Illustrative diagram of a piecewise linear hydropower production function with five sections

As discussed in the previous section, each triangular section is defined by three points of the form (q_j, h_j, p_j). Each section shares two common points with the section that precedes it as one moves in the $\hat{q}$ direction. These two points form a line that can be projected onto the (q_j, h_j) plane. The projection of the approximated HPF onto the (q_j, h_j) plane is shown in Figure 2-4 in blue. Using the relationship established in (2.21), the intersection of two adjacent sections is

$$q_j^{i,\min}(h_j) = \frac{\beta_j^{h,i} - \beta_j^{h,i-1}}{\beta_j^{q,i-1} - \beta_j^{q,i}} \cdot h_j + \frac{\beta_j^{0,i} - \beta_j^{0,i-1}}{\beta_j^{q,i-1} - \beta_j^{q,i}}. \tag{2.22}$$

These functions correspond to the lower and upper limits for the auxiliary variable q_j^i, or

$$q_j^{i,\min}(h_j) \le q_j^i \qquad q_j^i \le q_j^{i+1,\min}(h_j). \tag{2.23}$$

Since the approximated HPF is concave in the $\hat{q}$ direction, it is not necessary to add a mixed-integer or nonlinear constraint that ensures only one auxiliary variable q_j^i will not be equal to either its upper or lower boundary. However, such a mixed-integer constraint could be added to this formulation [21]. Note that in the case of the first section, the lower limit for q_j^1 is the minimum turbine discharge. Similarly, in the case of the last section I_j, the upper limit for $q_j^{I_j}$ is the maximum turbine discharge.

Total turbine discharge and generation

The total turbine discharge is the sum of all auxiliary turbine discharge variables minus their lower limits. Mathematically,

$$q_j = q_j^1 + \sum_{i=2}^{I_j} \left[q_j^i - q_j^{i,\min}(h_j) \right]. \tag{2.24}$$

A similar approach is used to compute total power production. Similar to the computation of $q_j^{i,\min}(h_j)$, we compute $p_j^{i,\min}(h_j)$ by projecting the linearized HPF onto the (p_j, h_j) plane. This projection is shown in Figure 2-4 in red. We can define the minimum power for section i of the hydropower production function as

$$p_j^{i,\min}(h_j) = \frac{\beta_j^{q,i}\beta_j^{h,i-1} - \beta_j^{q,i-1}\beta_j^{h,i}}{\beta_j^{q,i} - \beta_j^{q,i-1}} \cdot h_j + \frac{\beta_j^{q,i}\beta_j^{0,i-1} - \beta_j^{q,i-1}\beta_j^{0,i}}{\beta_j^{q,i} - \beta_j^{q,i-1}} \tag{2.25}$$

as a function of the hydraulic head h_j. Then, as in (2.24), the total power production is

$$p_j = p_j^1 + \sum_{i=2}^{I_j} \left[p_j^i(q_j^i, h_j^i) - p_j^{i,\min}(h_j) \right] \tag{2.26}$$

where p_j^i is calculated by (2.21). In other words, the total power production is the sum of the marginal power production from all sections of the linearized HPF. No constraints on p_j^i are necessary since it is a linear function of q_j^i and h_j, which are constrained by (2.18) and (2.23).

Optimization Problem

The state variables in our optimization model are the forebay elevation x_j, tailrace elevation z_j, and time delay variables $b_{j,m}$. The control variables are turbine discharge q_j, spill s_j, and natural inflow w_j. The MPC model is defined by relationships and (2.5) to (2.11). There are additional auxiliary turbine discharge and power variables for representing the approximated HPF. Finally, we introduce a power balance constraint

$$\sum_{j=1}^{J} p_j(k) = p_{\text{load}}(k) \quad \text{for } k = 0,1,\ldots,K-1 \tag{2.27}$$

where $p_{\text{load}}(k)$ is the forecasted net load satisfied by the cascade during a particular interval.

Our objective function is to minimize turbine discharge and spill. The objective function can be written as

$$\min_{q_j, s_j} \sum_{k=0}^{K-1} \sum_{j=1}^{J} \left[a_j \left(q_j(k) + a_j^0 \right)^2 + c_j \left(s_j(k) + c_j^0 \right)^2 \right] \tag{2.28}$$

where a_j and c_j are scalar weights, and a_j^0 and c_j^0 are scalar reference values. The quadratic program is convex if the scalar weights are non-negative.

Qualitatively, the goal of our coordinated control scheme is to minimize the amount of water needed to satisfy the system power balance, or (equivalently) to maximize the amount of stored water energy in the cascade. This is achieved by maximizing the effective hydraulic head $\tilde{h}$: the product of powerhouse efficiency η and hydraulic head h. If the turbine discharge of plant j is q_j, then the resulting change in effective hydraulic heads are

$$\Delta\tilde{h}_j = t_k \cdot \frac{\eta_j}{\Psi_j} q_j \qquad \Delta\tilde{h}_{j+1} = t_k \cdot \frac{\eta_{j+1}}{\Psi_{j+1}} q_j \tag{2.29}$$

where the upstream forebay elevation decreases and the downstream forebay elevation increases. In other words, for every one meter increase in the downstream forebay elevation, the upstream forebay elevation decreases according to the ratio

$$\frac{\Delta\tilde{h}_j}{\Delta\tilde{h}_{j+1}} = \frac{\eta_j}{\eta_{j+1}} \cdot \frac{\Psi_{j+1}}{\Psi_j}. \tag{2.30}$$

If the ratio is less than one (greater than one), then we can gain (lose) hydraulic head by discharging water from the upstream forebay to the downstream forebay. Using this ratio, we choose our weights such that

$$a_j = \left(\frac{\eta_j}{\eta_{j+1}} \cdot \frac{\Psi_{j+1}}{\Psi_j} \right)^2 \qquad a_j^0 = 0 \tag{2.31}$$

for $j = 1, \ldots, J$. We square the ratio because we are weighting q_j^2. In the case of the final dam in the cascade, there is no downstream forebay or HPP. Hence, we choose the weights a_J and a_J^0 large respective to the other weights on turbine discharge. Since we want to heavily penalize spill, we choose the weights c_j and c_j^0 very large. Weights used in our case study are given in the next section.

Case study

The coordination scheme developed in the previous sections was designed for the Mid-Columbia hydropower system. To demonstrate the efficacy of our scheme, we benchmarked the performance of our model to historical operations. The historical data was run through a state estimator to obtain turbine discharges that, when used as control inputs to the open-loop hydraulic model, resulted in forebay elevations that matched the historic values. Tailrace elevations were then computed using the developed tailrace model. Using the state estimated turbine discharges and hydraulic head, we then used local regression to compute the power production. Philosophically, if our coordination scheme computed the same control inputs as those used in historic system operations, the goal of the state estimation procedure was to ensure that the performance of our coordination scheme would be the same as that of the actual system operations.

Table 2-2
Simulation inputs and results, with elevations *x* given in meters, surface areas Ψ given in square meters, travel times τ in minutes, and energy given in MWh. The turbine discharge ramping score does not units, but a lower score indicates less ramping.

		System Parameters and Limits						Objective		Ramping			Net Energy	
		x^{min}	x^{max}	Ψ	η	τ	M	a	a^0	His.	Opt.	%	Pond	System
1	Grand Coulee	368.2	393.2	63	0.86	10	2	0.20	0	39.0	48.1	1.233	-5380	-5380
2	Chief Joseph	289.6	291.4	30	0.91	30	6	2.07	0	36.2	28.0	0.774	185	-5195
3	Wells	235.0	238.0	41	0.86	10	2	0.68	0	58.2	26.9	0.462	725	-4471
4	Rocky Reach	214.3	215.5	36	0.92	60	12	0.12	0	57.2	28.5	0.498	1586	-2884
5	Rock Island	185.6	186.8	12	0.86	45	9	22.92	0	68.1	21.5	0.315	715	-2170
6	Wanapum	171.9	174.2	57	0.86	90	18	0.24	0	72.6	12.0	0.166	1647	-523
7	Priest Rapids	146.8	148.1	28	0.87	45	9	100.00	10000	8.2	0.8	0.098	2231	1708

Hydraulic information about the Mid-Columbia system was determined and validated using the one- and five-minute datasets, including turbine discharges and limits, forebay elevations and limits, tailrace elevations, HPFs used to compute power production, water travel times, and reservoir surface areas. The total system load is shown in Figure 2-5. Natural inflow data, including flow into the Grand Coulee forebay, was compiled from streamflow data provided by the United States Geological Survey with 15-minute resolution [22]. These nature inflows on the Mid-Columbia River are usually a small percentage of the flow on the main stem river, and flow does not vary substantially on a minute-by-minute basis. Power forecasts were assumed to be perfect. System parameters and some results are given in Table 2-2.

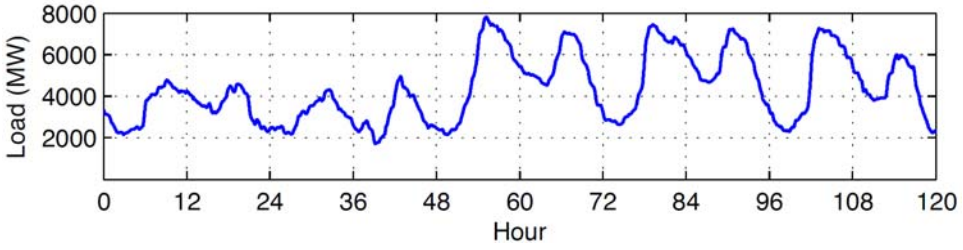

Figure 2-5
System load was significantly below system nameplate capacity during the simulation period.

We chose a period of five days (120 hours) in March 2013 for which we had one-minute Mid-Columbia operations data. We used an optimization interval t_k of five minutes, simulation interval of one minute, and time horizon K of four hours ($K = 48$). The coordination scheme determined a generation basepoint that was then mapped to a corresponding turbine discharge. In each simulation interval, the power balance was met while minimizing the deviation of each HPP from its basepoint and maintaining the feasibility of the system. Simulations were run on a desktop computer with an Intel Core 2 Duo 3.16 GHz and 4 GB of RAM running MATLAB 2012b (32-bit). We used the `qp-minos` solver called via the TOMLAB interface. The optimization problem consisted of 4,135 variables and 10,344 inequality constraints. The full simulation ran in 2:48:38 hours, or 7.44 seconds per optimization interval. This is an order of magnitude faster than comparable non-linear or mixed-integer optimization schemes.

We evaluated the performance of our coordination on four objectives: hydraulic potential, energy content, turbine discharge ramping, and the handling of system constraints.

Hydraulic potential. The objective function was designed to allocate water such that hydraulic head, or H/K, was maximized. Figure 2-6 shows that large forebays (e.g., Wanapum) were drafted in order to maintain hydraulic head at HPPs with small forebays (e.g., Priest Rapids). Total system H/K was 0.6% higher at the end of the simulation period, as shown in Figure 2-7. Hydraulic potential steadily increased during the study period, demonstrating how increased hydraulic potential results in lower flows which then results in increased hydraulic potential and so on.

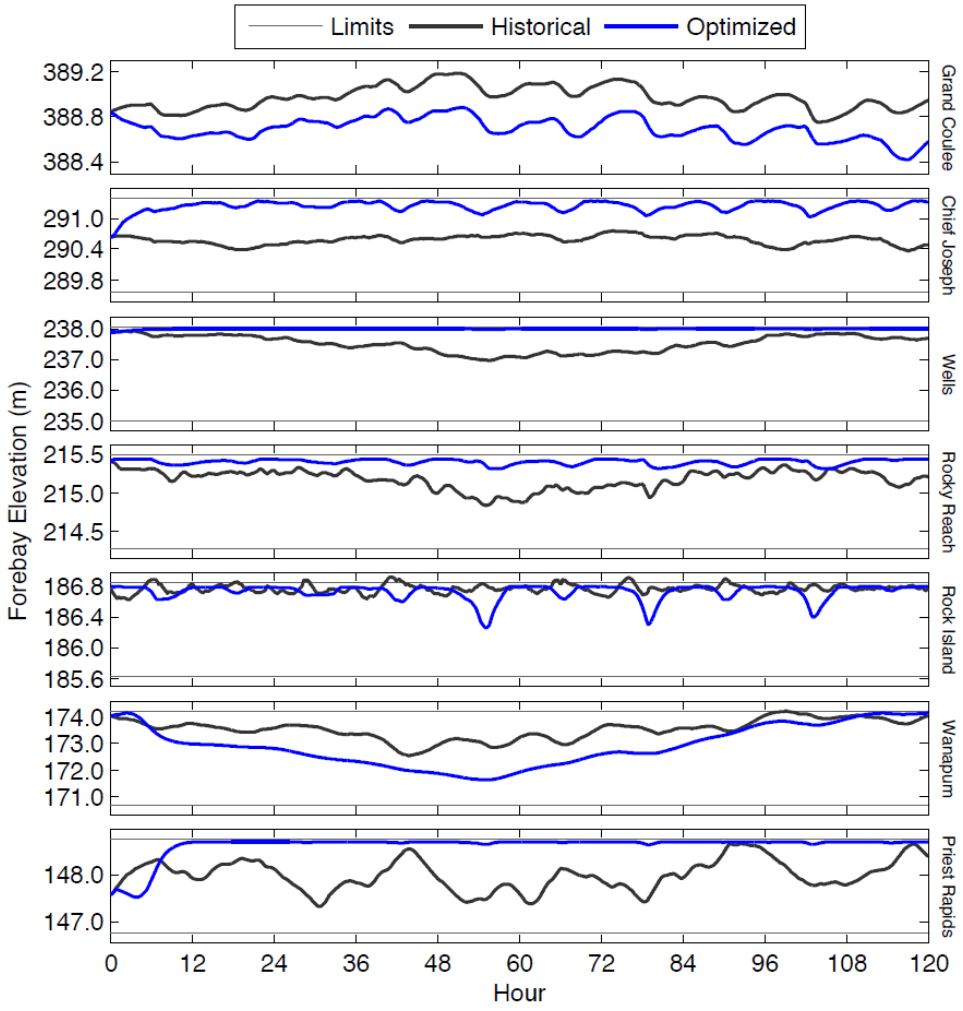

Figure 2-6
Forebays with small surface areas were kept full at the expense of forebays with larger surface areas. This strategy maximizes the hydraulic potential of the system.

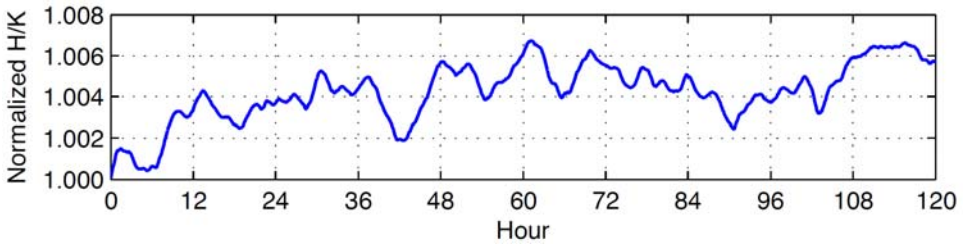

Figure 2-7
Hydraulic potential, or H/K, increased steadily over the course of the five-day simulation period, ending approximately 0.6% greater.

Energy. Net energy stored in the cascade is the total stored energy in the cascade in the optimized case minus total stored energy in the cascade in the historical case. The energy stored in a single reservoir accounts for the water stored in that reservoir and the upstream reservoirs. This accounts for the fact that water in upstream HPPs must still be discharged through the downstream HPPs and is therefore inherently more valuable. Mathematically,

$$E_j(n) = \frac{\sum_{m=1}^{n} p_j(m)}{\sum_{m=1}^{n} q_j(m)} \cdot \sum_{i=1}^{j} \Psi_j \left(x_i^{\text{opt}}(n) - x_i^{\text{hist}}(n) \right) \tag{2.32}$$

where $E_j(n)$ is the energy stored in reservoir j at time n. System energy is the running sum of reservoir energies. In Table 2-2, these values are referred to as pond and system energy, respectively. As shown in Table 2-2 and illustrated in Figure 2-8, all HPPs ran an energy surplus except for Grand Coulee. Grand Coulee's forebay was drafted to supply the water to the downstream projects, as shown in Figure 2-6. Overall, the net energy benefit was 1708 MWh, or 0.33% of the total energy produced during the five day simulation period.

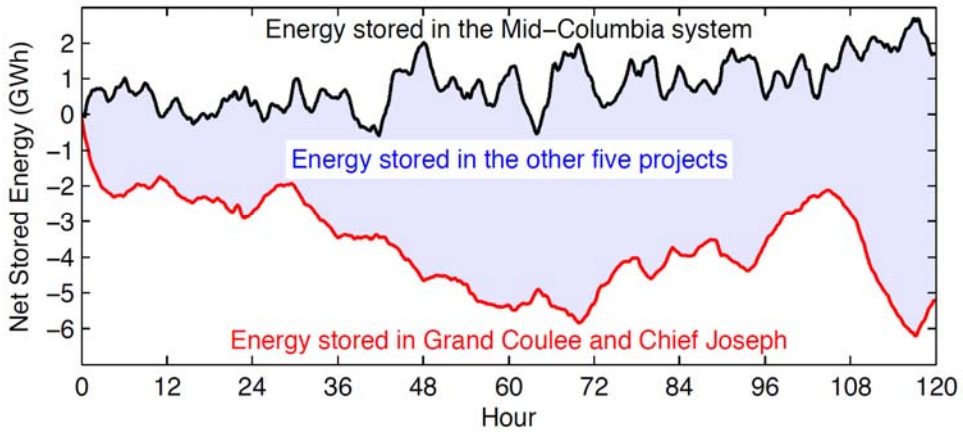

Figure 2-8
The energy deficit at Grand Coulee Dam was compensated by energy surpluses at the remaining six dams. The total net energy stored was positive.

Ramping. Ramping was reduced and turbine discharges had smoother profiles. Ramping was highest at Grand Coulee and lowest at Wanapum and Priest Rapids, as shown in Figure 2-9. Quantitative analysis shown in Table 2-2 corroborated the qualitative observation that ramping was reduced according to the location of the HPP in the cascade. Rampign scores are computed from the sum of the absolute change in turbine discharge at each time step; scores were calculated on smoothed turbine discharge data to remove the measurement and process noise in the historical data. The reduction in ramping was not an explicit optimization objective, but the behavior emerged from the quadratic objective function and the chosen weights.

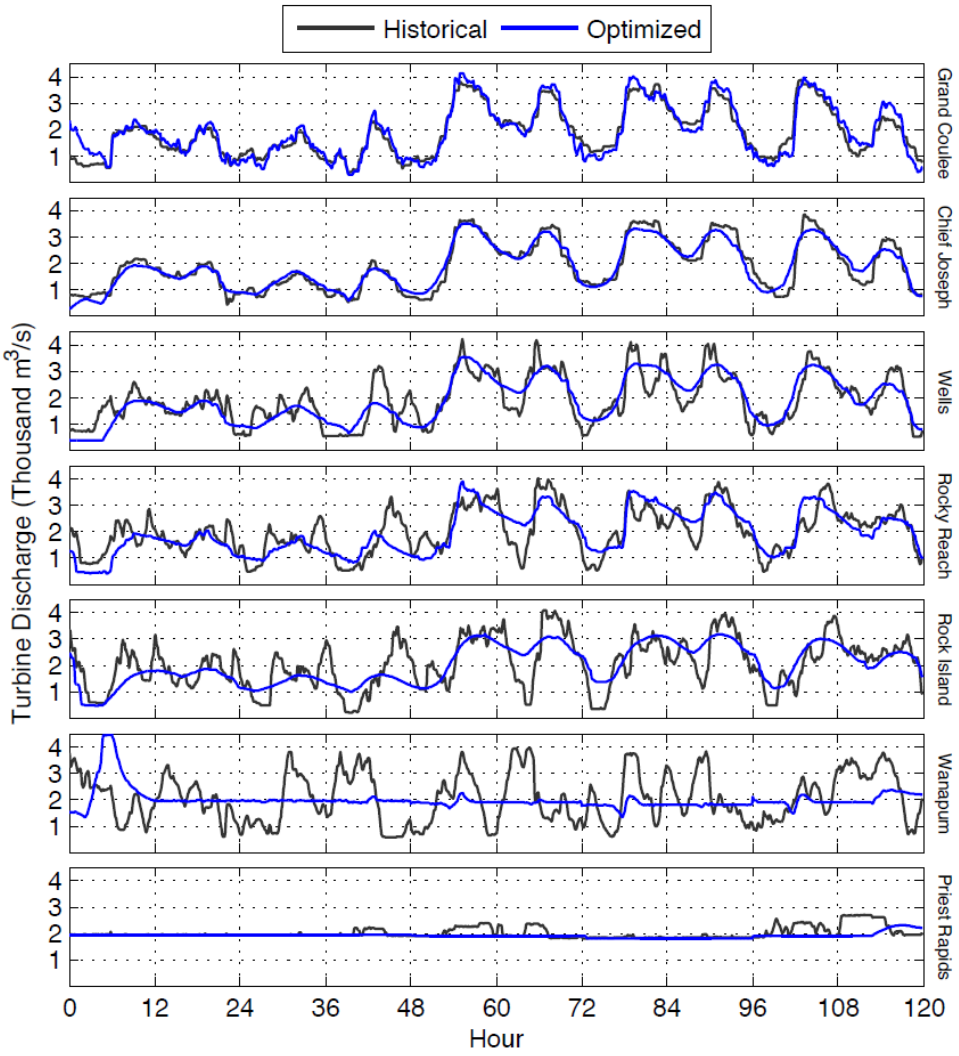

Figure 2-9
Ramping of turbine discharges was significantly reduced using the proposed coordination scheme.

System constraints. We focus on one particular constraint, where Priest Rapids had a minimum discharge limit of 1900 m^3/s. Priest Rapids experienced reverse load factoring, generating a larger share of energy during off-peak hours, as shown in Figure 2-10. Since we placed a heavy penalty on turbine discharge from Priest Rapids, Wanapum was drafted in order to maintain a full forebay at Priest Rapids and maintain maximum generation efficiency. This was the behavior we expected to see. The Mid-Columbia is heavily constrained by environmental regulations on flow, so the fact that the flow constraint at Priest Rapids was incorporated satisfactorily bodes well for the performance prospects of our coordination scheme in other scenarios.

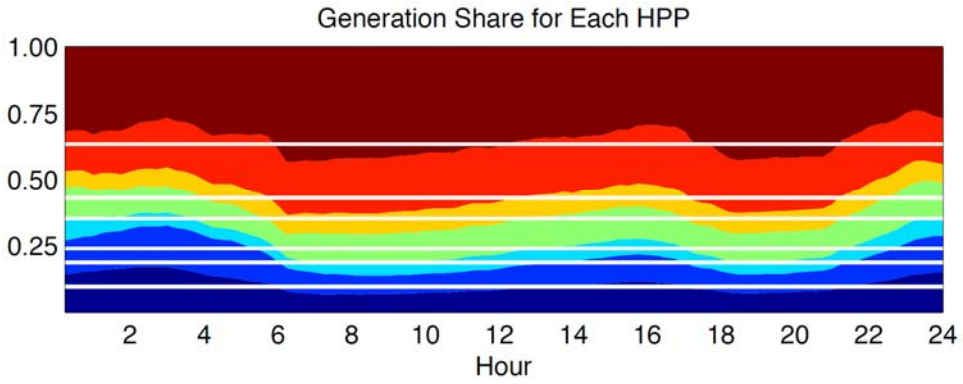

Figure 2-10
The high minimum discharge limit at Priest Rapids Dam resulted in Priest Rapids generating a larger share of the system generation during off-peak hours. Grand Coulee is on the top of the plot. Chief Joseph is below Grand Coulee, and so on. Priest Rapids is on the bottom of the chart. The white lines indicate the generation share if turbine discharge through each HPP was identical.

Conclusion

This section presented a coordinated control scheme for the Mid-Columbia hydropower system. Our hydraulic model consisted of the water balance equation (including water travel times) and a model of tailrace dynamics. We approximated the hydropower power production function using a piecewise planar function that can be written as a set of linear constraints. This approximation accounts for head effects and non-constant efficiency. The objective function was formulated to allocate water such that the total hydraulic head of the system was maximized. We compared the performance of our control scheme to the historical operation of the Mid-Columbia system. The results showed that our control scheme minimized ramping, increased system hydraulic head, increased the energy stored in the cascade, and successfully handled system constraints. Future work includes the analysis of different objective functions that maximize water use efficiency, and the assessment of our scheme under different load and constraint scenarios. We also intend to study how the approximated HPF might be incorporated when the objective function causes the approximated HPF to be evaluated incorrectly (i.e., when the objective is to minimize something other than turbine discharge and spill). Additionally, we plan to use this control framework to analyze the ability of the municipal dams located on the Mid-Columbia river to balance the wind generation variability.

References

1. L. Rux, “An incremental economic dispatch method for cascaded hydroelectric power plants,” *IEEE Transactions on Power Systems*, Vol. 8, No. 3, pp. 126-1273 (August 1993).

2. P.-H. Chen and H.-C. Chang, “Genetic aided scheduling of hydraulically coupled plants in hydro-thermal coordination,” *IEEE Transactions on Power Systems*, Vol. 11, No. 2, pp. 975-981 (May 1996).

3. H. Habibollahzadeh and J. A. Bubenko, “Application of decomposition techniques to short-term operation planning of hydrothermal power system,” *IEEE Transactions on Power Systems*, Vol. 1, No. 1, pp. 41-47 (February 1986).

4. O. Nilsson and D. Sjelvgren, "Mixed-integer programming applied to short-term planning of a hydro-thermal system," *IEEE Transactions on Power Systems*, Vol. 11, No. 1, pp. 281-286 (February 1996).

5. A. Conejo, J. Arroyo, J. Contreras, and F. Villamor, "Self-scheduling of a hydro producer in a pool-based electricity market," *IEEE Transactions on Power Systems*, Vol. 17, No. 4, pp. 1265-1272 (November 2002).

6. J. Catalao, S. J. P. S. Mariano, V. Mendes, and L. A. F. M. Ferreira, "Scheduling of head-sensitive cascaded hydro systems: a nonlinear approach," *IEEE Transactions on Power Systems*, Vol. 24, No. 1, pp. 337-346 (February 2009).

7. S. M. Amado and C. C. Ribeiro, "Short-term generation scheduling of hydraulic multi-reservoir multi-area interconnected systems," *IEEE Transactions on Power Systems*, Vol. 2, No. 3, pp. 758-763 (August 1987).

8. J. Matevosyan, M. Olsson, and L. Söder, "Hydropower planning coordinated with win power in areas with congestion problems for trading on the spot and the regulating market," *Electric Power Systems Research*, Vol. 79, No. 1, pp. 39-48 (January 2009).

9. A. Hamann and G. Hug, "Real-time optimization of a hydropower cascade using a linear modeling approach", presented at the Power Systems Computation Conference (PSCC), Wrocław, Poland (August 2014).

10. W. T. Alley, "Hydroelectric plant capability curves," *IEEE Transactions on Power Apparatus and Systems*, Vol. 96, No. 3, pp. 999-1003 (May 1977).

11. A. Arce, T. Ohishi, and S. Soares, "Optimal dispatch of generating units of the Itaipu hydroelectric plant," *IEEE Transactions on Power Systems*, Vol. 17, No. 1, pp. 154-158 (February 2002).

12. A. L. Diniz and M. E. P. Maceira, "A four-dimensional model of hydro generation for the short-term hydrothermal dispatch problem considering head and spillage effects," *IEEE Transactions on Power Systems*, Vol. 23, No. 3, pp. 1298-1308 (August 2008).

13. R. Lima, M. Marcovecchio, A. Novais, and I. Grossman, "On the computational studies of deterministic global optimiziation of head dependent short-term hydro scheduling," *IEEE Transactions on Power Systems*, Vol. 28, No. 4, pp. 4336-4347 (November 2013).

14. M. Cordova, E. Finardi, F. Ribas, V. de Matos, and M. Scuzziato, "Performance evaluation and energy production optimization in the real-time operation of hydropower plants," *Electric Power Systems Research*, Vol. 116, pp. 201-207 (November 2014).

15. I. Hidalgo, D. Fontane, M. Arabi, J. Lopes, J. Andrade, and L. Ribeiro, "Evaluation of optimization algorithms to adjust efficiency curves for hydroelectric generating units," *Journal of Energy Engineering*, Vol. 138, No. 4, pp. 172-178 (December 2012).

16. B. Papillon and T. Freeman, "Rehabilitating the Francis units at Chief Joseph," *Hydro Review*, Vol. 32, No. 8 (October 2013).

17. L. H. Sheldon, “Optimizing the generating efficiency of entire powerhouses,” presented at HydroVision 2008, Sacramento, California (July 2008).

18. X. Li., T. Li, J. Wei, G. Wang, and W.-G. Yeh, “Hydro unit commitment via mixed integer linear programming: a case study of the Three Gorges Project, China,” *IEEE Transactions on Power Systems*, Vol. 29, No. 3, pp. 1232-1241 (May 2014).

19. B. Tong, Q. Zhai, and X. Guan, “An MILP based formulation for short-term hydro generation scheduling with analysis of the linearization effects on solution feasibility,” *IEEE Transactions on Power Systems*, Vol. 28, No. 4, pp. 3588-3599 (November 2013).

20. S. Weisberg. *Applied Linear Regression*. 3rd ed. Wiley-Interscience, Hoboken, New Jersey 2005.

21. J. Garcia-Gonzalez and G. Castro, “Short-term hydro scheduling with cascaded and head-dependent reservoirs based on mixed-integer linear programming,” presented at PowerTech 2011, Porto, Portugal (2001).

22. United States Geological Survey. USGS current water data for USA. [Online]. Available: http://waterdata.usgs.gov/usa/nwis/rt

3 Simulation of a Hydropower Cascade Using Historical Data and State Estimation

Introduction

Controller design for physical systems consists of several phases. The physical system must first be characterized in order to make engineering decisions about which attributes and relationships are important and which can be ignored. These attributes and relationships are used to derive a model according to whatever model properties are important (e.g., linear or non-linear, time-invariant or time-varying, causal or non-causal). More complicated models will (generally) more accurately reflect the behavior of the system, but fitting additional parameters can be difficult without adequate information. The validity of the model can be evaluated by analyzing how closely the output of the model corresponds with the output of the physical system, assuming both the model and the physical system have been excited with the same set of control inputs. Once the model has achieved a satisfactory level of accuracy, a controller can then be built or a control scheme can be devised based on that developed model. The performance of the controller is generally assessed first via computer simulation and then by testing it on the physical system.

For systems where the physical system is well-known and models of varying complexity can be developed from first principles (i.e., physical laws), simulation can be done with a reasonable degree of accuracy. Then, the controller can be tested using computer simulation, and the engineering process of revising and testing the design can begin. However, in hydropower, there are several factors that combine to make the simulation and validation of control schemes difficult. First, developing an accurate higher-order hydraulic model is difficult. Anything beyond a basic linear model requires using equations describing open-channel flow, equations that are parameterized by the physical characteristics of the river basin in which the hydropower system operates. Hence, running an open-channel flow model is expensive from a computational, financial, and data perspective.

This leads to the second problem, wherein the system hydraulics model must be reconciled with measurements of system inputs (e.g., flows) and outputs (e.g., forebay elevations). Flow meters are notoriously noisy and biased, hence measurements of turbine discharge or inflow cannot be completely trusted. Forebay elevation measurements are fairly accurate, but their precision cannot be trusted beyond the centimeter level. The changes in forebay elevation from one time step to the next (for a simulation with sub-hourly resolution) are thus much smaller than the range of precision in the forebay elevation measurement. Hence, there are two types of measurements: one cannot be trusted because it could possibly be biased, and the other is of limited use because it is noisy.

Third, and lastly, is the problem of comparing a new control scheme with the historical operations of the hydropower cascade or of an alternate control scheme. In order to do that, we need assurances that our model reflects what would happen to the state of the hydropower system given a certain sequence of control actions. In doing that, we would simulate the system using the given control inputs and compare the output to the measured system state. This would imply that any observed inaccuracies are the result of an incorrect model. However, if we accept the conceit that the model is accurate (or at the very least as good as it can be) and the

measurements are inaccurate, then the problem is how to adjust the measured control inputs and system states to the hydraulic model. This problem is known as state estimation.

This section discusses the state estimation procedure we developed. The goal of this procedure is to create a simple, effective approach to reconcile noisy, biased discharge measurements with the measurements of the true system state (forebay elevation) and the inherent inaccuracy of the hydraulic model. As noted before, in the absence of enough data to properly characterize a more sophisticated open-channel flow model, we elected to use a linear hydraulic model for both the simulation and optimization of the Mid-Columbia system. We assume that measurements of forebay elevation are noisy but unbiased, and hence the forebay elevation should, over time, reflect the trajectory of the true forebay elevation. We assume that flow measurements (either inflow or outflow) are biased and noisy and can only be trusted to the extent that they represent the shape of the discharge profile. In other words, if the measured outflow doubles, then it is reasonable to expect that the estimated outflow should also (roughly) double. The objective is to estimate the flows at various points in the system and then use those flow estimates to create an estimated open-loop forebay elevation for each dam. Estimated flow and elevation values should track the measured values closely.

There are two general approaches to state estimation [1]. The first of these is least-squares. This procedure entails minimizing the squared residual error between the estimated value and the measured value. It is an optimization-based approach. The estimated variables are related to each other by a state-space model or something similar. There are two problems with using least-squares for estimating the flows and forebay elevations in a hydropower system. First, how should the objective function be formulated? Each measurement should not be trusted the same, but it is not known *a priori* which measurements are less biased or less noisy. Second, how do we deal with the scale of the problem? Estimating only the flows through the seven dams in the Mid-Columbia system for a week with 1-minute time resolution would require 70,560 variables. Solving such a problem directly is difficult even in the unconstrained case. A hydropower system that has strong temporal and spatial coupling only exacerbates the difficulty of computing an optimal solution.

The other approach for state estimation is Kalman filtering. The Kalman filter will derive the statistically optimal estimate of the underlying system state from measurements of the system inputs and outputs [2]. Kalman filtering is typically employed in cases where the internal system state is hidden from the observer and cannot be directly measured. In light of these facts, we applied the Kalman filter to a theoretical case where the forebay elevation of a hydropower system was known with some certainty and the flow measurements were noisy but unbiased. The Kalman filter did an excellent job at estimating both the flows and forebay elevations in the system; the computational simplicity of the Kalman filter was also appealing. However, when we used the Kalman filter to estimate historical flows using historical measurements of forebay elevation (noisy but unbiased) and flows (biased as well as noisy), the Kalman filter did a poor job of removing the bias from the flow measurements, and the estimates were erratic and (qualitatively) suboptimal.

Our difficulties implementing those two estimation approaches lead us to seek another solution. The overall objective was not to create a statistically or mathematically optimal estimator. Rather, we wanted to engineer a functional, simple, and fast algorithm to make all these measurements fit together. The remainder of this section describes that engineering process.

"Mid-Columbia Hydropower System" introduces the Mid-Columbia hydropower system. "The Need for State Estimation" outlines the need and rationale for state estimation in a hydropower system. "State Estimation" describes the proposed state estimation procedure. "Overview and Results" presents some example results from the Mid-Columbia hydropower system. "Conclusion" concludes the section.

Mid-Columbia Hydropower System

Our primary research focus is on the coordinated control and optimization of the Mid-Columbia hydropower system. The Mid-C consists of seven dams on the Columbia River in Washington: two federal dams (Grand Coulee and Chief Joseph) and five municipal dams. The first dam in the cascade is Grand Coulee; the last dam in the cascade is Priest Rapids. Figure \ref{fig:map} shows a map of the hydropower facilities in the Columbia River Basin, with the seven Mid-C dams visible in the middle of the figure.

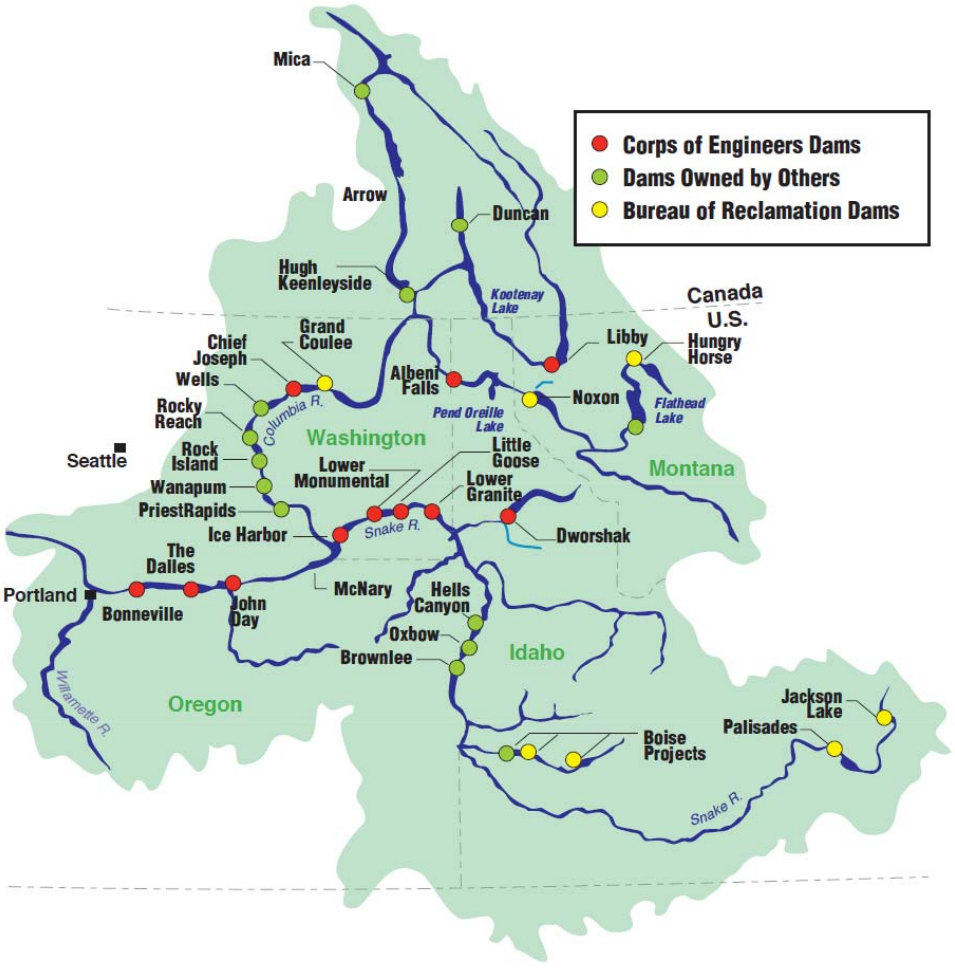

Figure 3-1
Map of hydropower installations in the Columbia River Basin (Source: USACE)

This state estimation procedure was borne from a need to compare the historical operations of the Mid-C with the coordinated control scheme that we developed. We were provided with turbine discharge and spill measurements, along with readings of forebay elevation. We used

data from the USGS for the inflow into the Lake Roosevelt (the reservoir behind Grand Coulee Dam). In order to properly compare our proposed control scheme with historical operations, we had to be able to simulate the system. Unfortunately, many of the flow measurements are biased and disagree with each other. In some cases, the total inflow into a reservoir was several percent higher than the outflow from that reservoir. When simulating a system using open-loop simulation (i.e., without being able to measure the "true"' state of the physical system), these measurements need to be massaged so that the open-loop simulation of the physical system matches the responses of the actual physical system.

This section is focused entirely on the state estimation procedure that takes this historical data and estimates a set of estimated turbine discharges and forebay elevations, thus permitting a true apples to apples comparison of the proposed coordinated control scheme and the historical operations of the Mid-Columbia system. This procedure should be useful to other researchers doing similar kinds of hydropower operations and planning work, where the need to do accurate backcasting simulations on a computer is required.

The Need for State Estimation

In control theory, a linear, time-invariant, discrete-time state space model has the general formulation

$$\mathbf{x}(k+1) = A\mathbf{x}(k) + B\mathbf{u}(k) \tag{3.1}$$

where the system has been discretized by the discretization interval t_k. The A and B matrices describe the relationship between the control inputs $\mathbf{u}(k)$, current system state $\mathbf{x}(k)$, and future system state $\mathbf{x}(k+1)$. The state-space formulation of control problems is useful because the mathematical relationship between the control inputs and changing system state can be analyzed and implemented in a transparent manner. Its linearity properties make it ideal for use in an optimization-based controller framework (e.g., model predictive control). In a hydropower cascade, the system state is generally the forebay elevation or the volume of water in storage. The control inputs are the flows at various points in the system. A and B reflect how those flows affect the water stored at various locations in the system.

In lieu of analyzing a large, multi-reservoir system in one go, first consider the state space model for a single hydropower plant impounding a single reservoir. The system state is represented by the forebay elevation $x(k)$. The control variables are the reservoir inflow and outflow. The state space representation for this model is

$$x(k+1) = x(k) + \frac{t_k}{\Psi} r(k) - \frac{t_k}{\Psi} q(k) \tag{3.2}$$

where r is the inflow, q is the outflow, and Ψ is the surface area of the reservoir. We make the explicit and reasonable assumption that the volume of water in the forebay is linearly related with the elevation of the forebay. We also make the assumption that the inflow is known with certainty; this assumption is critical to the proposed state estimation procedure. (This process can easily be reversed such that the outflow is known with certainty, and the inflow is the unknown quantity.) Since we know (and trust) the measurements of forebay elevation $x(k)$ and $x(k+1)$,

we therefore know three of the four unknowns in (3.2). Since this is an equality constraint, the fourth unknown (implied outflow) can be computed as

$$\bar{q}(k) = \frac{\Psi}{t_k} x(k) - \frac{\Psi}{t_k} x(k+1) + r(k) \tag{3.3}$$

where the implied outflow is denoted by $\bar{q}$. Then, there are two "measurements" of outflow: the directly measured outflow q and the outflow $\bar{q}$ implied by the measurements of forebay elevation and inflow. The problem of state estimation is how to reconcile these two conflicting measurements into an estimated outflow $\hat{q}$.

Our approach is based around two guiding principles. First, while the measured outflow is biased, noisy, and will probably not satisfy the water equation, it contains information about the "shape" of the outflow signal that we want to preserve. Second, the integral of the implied outflow signal represents the water balance that the estimated outflow needs to satisfy, but the shape of the implied outflow signal is substantially different from the measured outflow signal. Hence, while the implied outflow cannot be used directly, its integral can be used to adjust the measured outflow such that the water balance is satisfied. These two principles thus inform our general state estimation approach: use the implied outflow to debias the measured outflow. This will satisfy the water balance equations while also preserving information about turbine ramping.

To demonstrate how we implement this approach, consider the simple case where there is a constant, negative bias in the outflow measurements (e.g., the measured outflow is always one kcfs below the actual outflow). In this case, the accumulated discharge of the implied outflow would be higher than the accumulated discharge of the measured outflow. This accumulation would be proportional to both the bias and how much time has elapsed since the initial system state was recorded. In simulation, this would manifest itself in a simulated forebay elevation higher than the measured forebay elevation, since less outflow is simulated than what actually occurred.

An example of this scenario is shown in Figure 3-2. The black line is the accumulated discharge for the measured outflow assuming a zero-order hold on the discrete outflow measurements, or

$$v(k) = t_k \sum_{n=1}^{k} q(n). \tag{3.4}$$

The blue line is the accumulated discharge for the implied outflow, or

$$\bar{v}(k) = t_k \sum_{n=1}^{k} \bar{q}(n). \tag{3.5}$$

The values computed in (3.4) and (3.5) are water volumes. Since there was a negative bias in the outflow measurement, the blue line is located above the black line. If we call the bias q^0 and subtract (3.4) from (3.5), then

$$
\begin{aligned}
\bar{v}(k) - v(k) &= t_k \sum_{n=1}^{k} \bar{q}(n) - t_k \sum_{n=1}^{k} q(n) \\
&= t_k \sum_{n=1}^{k} \left(q(n) + q^0 \right) - t_k \sum_{n=1}^{k} q(n) \\
&= t_k \sum_{n=1}^{k} q^0 + t_k \sum_{n=1}^{k} q(n) - t_k \sum_{n=1}^{k} q(n) \\
&= t_k \sum_{n=1}^{k} q^0 \\
&= t_k \cdot q^0 \cdot k.
\end{aligned}
\tag{3.6}
$$

This is a linear function, and is shown as the red line in Figure 3-2. We call this function $d(k)$, or the "difference function". It is defined as

$$
d(k) = t_k \left(\sum_{n=0}^{k-1} \bar{q}(n) - \sum_{n=0}^{k-1} q(n) \right). \tag{3.7}
$$

If $d(k)$ is positive, the flow measurements are negatively biased and the outflow should be adjusted upwards. If $d(k)$ is negative, the flow measurements are positively biased and the outflow should be adjusted downwards. Since the summation is from 0 to $k-1$, we define $d(0) = 0$.

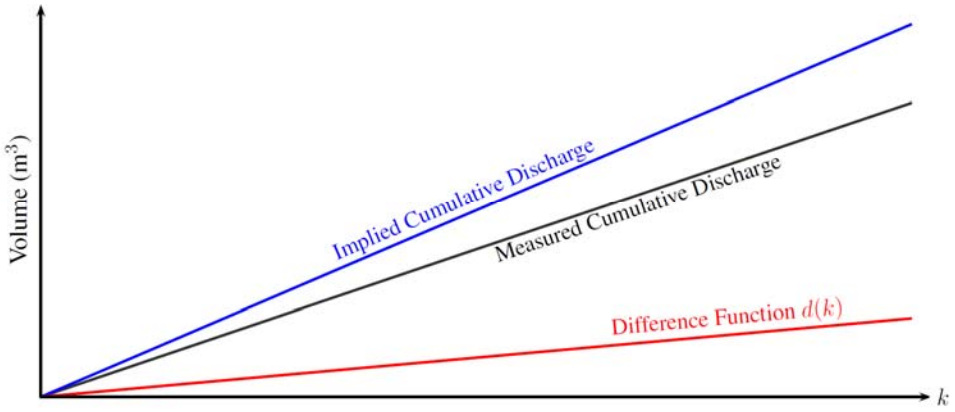

Figure 3-2
Schematic illustrating how a biased outflow manifests itself as a differene between the cumulative measured discharge and the cumulative implied discharge

In this contrived example, removing the bias from the outflow measurements is simple subtraction. In real applications—even if the difference function was noisy but followed a linear trend—we would be best served by fitting a linear regression to the data and using that to remove the bias in the measured outflow. In practice, however, the bias value q_0 is not constant. Rather, it can fluctuate across the simulation period of interest (days or weeks). The next section steps through how we formulated the problem, discusses some of the challenges we encountered, and details the solutions we engineered to overcome them.

State Estimation

Estimating the difference function using linear regression

As discussed previously, a constant bias would result in a linear bias function, which can be estimated using a linear regression of the form

$$\hat{d}(k) = \hat{\beta}k \tag{3.8}$$

where one parameter is fitted to the model. There is no intercept parameter because $\hat{d}(0) = d(0) = 0$. (A non-zero initial value for the difference function would not have any physical meaning.) The optimization problem would then be

$$\min_{\hat{d}(k)} \left\{ \sum_{k=1}^{K} \left(\hat{d}(k) - d(k) \right)^2 \right\} \Leftrightarrow \min_{\hat{\beta}} \left\{ \sum_{k=1}^{K} \left(\hat{\beta}k - d(k) \right)^2 \right\} \tag{3.9}$$

where $d(k)$ is defined for all $k = 0, \ldots, K$. This is an unconstrained, convex, quadratic programming problem and can be solved in closed-form.

To discuss how we improved on this basic regression, we are going to walk through the estimation of the inflow into the Grand Coulee forebay. In our system-level state estimation, we assume that the turbine discharge from Grand Coulee is the "true" discharge of the system. (In practice, any plant could have been chosen, and the state estimation procedure would not change.) Hence, we work our way upstream to estimate inflows, and we work our way downstream to estimate outflows. Thus, the inflow into the Grand Coulee forebay is the first quantity to be estimated. The measured inflow was taken from a USGS river gauge located on the Columbia River at the Canadian border [3]. The implied inflow was computed from the turbine discharge measurements taken at Grand Coulee and the forebay elevation measurements. (As noted before, the procedures for estimating inflow as opposed to outflow are nearly identical.) Inflow data was available with 15-minute time resolution and forebay elevation data was available with 5-minute time resolution. Turbine discharge data was available with 1-minute time resolution, hence all estimation was done on a 1-minute time resolution. The inflow and forebay elevation measurements were upsampled using linear interpolation. Data was taken for a five-day period in March 2013.

Figure 3-3 shows two columns of five plots each. The first column of plots shows the function $\hat{d}(k)$ (in red) regressed on the true difference function (in black). Previously fit functions are shown in grey. The second column of plots shows the derivative of $\hat{d}(k)$, or the estimated bias function (i.e., the adjustment made to the measured flow in order to obtain the estimated flow). For a linear regression, the estimated bias will be a constant value. For a higher-order regression, the estimated bias will change with time.

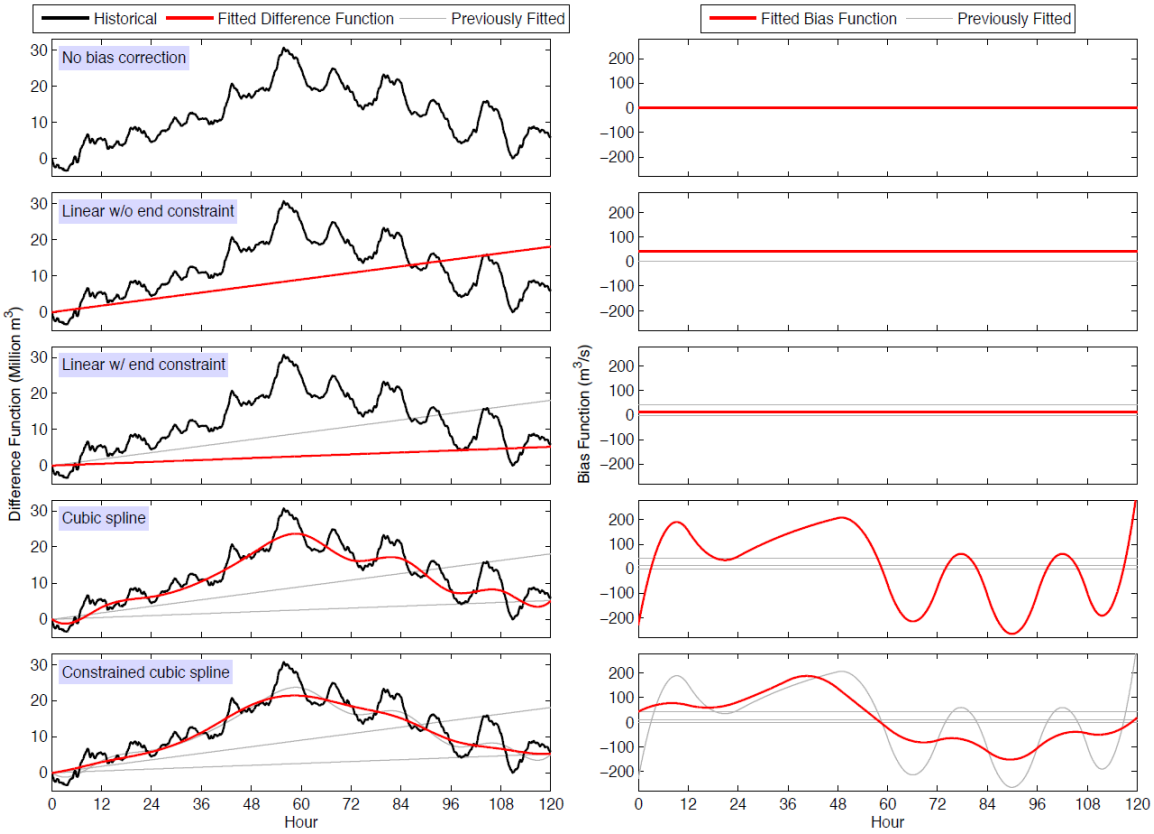

Figure 3-3
These plots pertain to the estimation of the inflow into the Grand Coulee forebay. The left column of plots shows the difference function in black and the fitted difference function in red. The right column shows the derivative of the fitted difference function, which can be interpreted as the bias. In order from top to bottom, the rows show the results for no correction, linear difference function, linear difference function with water balance constraint, cubic spline, and cubic spline with ramping constraint. The knots for the cubic spline were located at each 12-hour interval (i.e., the tick marks on the x-axis).

The first row of data shows the uncorrected difference function. Its corresponding bias function is zero. The second row of data shows the difference function approximated using the linear regression described in (3.8). Looking at the difference function and its corresponding linear regression, we immediately notice two problems. First, the difference function is not linear. We are regressing a linear function onto a set of data that is clearly not linear. Second, the difference function does not obey the water balance.

As noted before, the cumulative implied inflow and the cumulative estimated inflow should be the same in order for the water balance equation to hold. This problem is illustrated in Figure 3-4, which shows two columns of five plots each. The first column of plots shows the measured forebay elevation (in black), the open-loop forebay elevation using the measured inflow (in grey), and the open-loop forebay elevation using the estimated inflow (in red). The open-loop forebay elevation is simulated by taking the system state at $k = 0$, applying the control inputs (i.e., inflow and outflow) for $k = 0,\ldots,K-1$, and observing the trajectory of the system state for $k = 1,\ldots,K$. In normal operations, there would be feedback on the system state because the system state would be measured in real-time. In simulation, those measurements are not available, hence we can only rely on open-loop simulation to model our system.

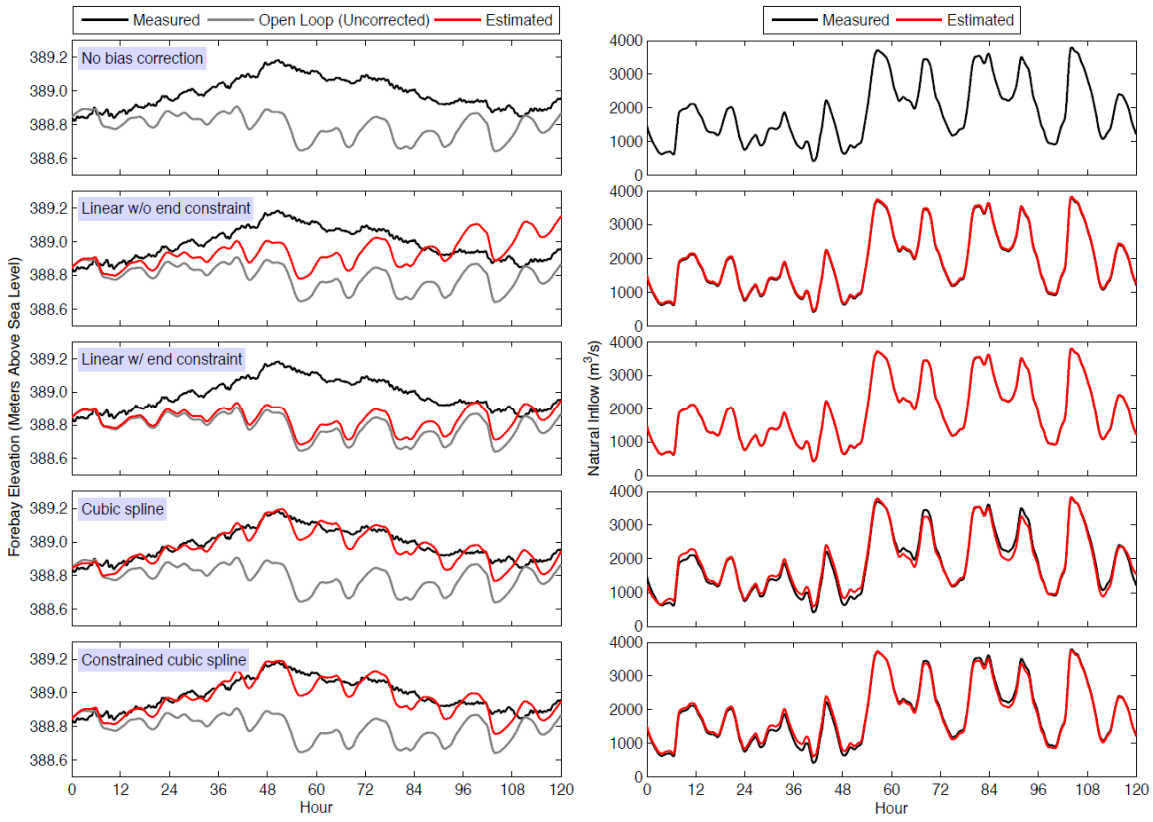

Figure 3-4
These plots pertain to the estimation of the inflow into the Grand Coulee forebay. The left column of plots shows the measured forebay elevation in black, the open-loop forebay elevation using the measured inflow in grey, and the open-loop forebay elevation using the estimated discharge in red. The right column shows the measured inflow in black and the estimated inflow in red. In order from top to bottom, the rows show the results for no correction, linear difference function, linear difference function with water balance constraint, cubic spline, and cubic spline with ramping constraint.

The first row of data shows the forebay elevation and inflow when $\hat{d}(k) = 0$ for all k (i.e., the uncorrected case). Looking at the left plot of forebay elevation, the open-loop forebay elevation does not track the measured forebay elevation very well, implying that the underlying difference function is not linear. As mentioned before, the water balance is not satisfied; if it was, the measured forebay and estimated forebay elevations would be identical when $k = K$. Hence, there are two problems that need to be addressed. First, how do we enforce the water balance constraint? Second, how do we deal with the non-linearity in the difference function?

Enforcing the water balance constraint

Addressing the first problem is fairly simple. Since the water balance will only be satisfied when $\hat{d}(K) = d(k)$, then the optimization problem in (3.9) is adjusted to be a constrained optimization problem of the form

$$\min_{\hat{\beta}} \left\{ \sum_{k=1}^{K} \left(\hat{\beta} k - d(k) \right)^2 \right\} \tag{3.10}$$

subject to

$$\hat{d}(K) = \hat{\beta}K = d(k). \tag{3.11}$$

However, this problem is clearly trivial. Since there is no intercept parameter, there is already an implicit constraint that $\hat{d}(0) = d(0) = 0$. We added the constraint $\hat{d}(K) = \hat{\beta}K = d(k)$. Since this is a linear regression with one parameter, this optimization merely fits a line between $d(0)$ and $d(K)$. The results of this regression are shown in the third row of Figure 3-3 and Figure 3-4. The difference function fit using the above optimization problem is provably inferior to the linear regression fit using (3.9). In return for this reduction in accuracy, however, the water balance is strictly maintained for the simulation period.

Accomodating nonlinearity

Hence, one of the problems is satisfied. In solving that problem, however, an additional issue arises: how do we add additional degrees of freedom to our regression such that we are doing more than just connecting $d(0)$ and $d(K)$ with a straight line? Luckily, addressing this problem will also deal with the previously identified problem of regressing a nonlinear difference function. There are multiple ways to do regression with higher-order terms (e.g., fitting a quadratic or cubic function, piecewise linear functions, etc.) or explicit nonlinear/nonparametric regression (e.g., kernel regression, LOESS, generalized linear models, etc.) [4]. We elected to use cubic splines.

Cubic splines are piecewise cubic functions with continuity and smoothness constraints. To fit a cubic spline, N knots (or breakpoints) are chosen prior to doing the regression. The location of a knot is denoted by ξ_n. Since the parameter of interest is the discrete-time index variable k, each ξ_n will be a time index. Then, a total of $N+1$ cubic functions are fit to the data, with one cubic function defined between each knot. Each data point is then assigned to a particular region, and its estimated value is computed using the appropriate cubic function. Smoothness and continuity constraints are enforced at each knot (i.e., the function and its first two derivatives are equal at each knot). Mathematically, splines can be defined as

$$f(x) = \hat{\beta}_{3,n}x^3 + \hat{\beta}_{2,n}x^2 + \hat{\beta}_{1,n}x + \hat{\beta}_{0,n} \quad \forall x \in [\xi_{n-1}, \xi_n] \tag{3.12}$$

where there are four β's fit to each region of the regression. Since there are N knots and $N+1$ regions where each cubic function is valid, there are a total of $4N+4$ parameters fit to the model. It is assumed that $\xi_0 = 0$ and $\xi_{N+1} = K$.

Using cubic splines, the state estimation optimization problem can then be written

$$\min_{\hat{\beta}} \left\{ \sum_{k=1}^{K} \left(\hat{d}(k) - d(k) \right)^2 \right\} \tag{3.13}$$

subject to

$$\hat{d}(k) = f(k) \tag{3.14}$$

$$\hat{d}(0) = \hat{\beta}_{1,0} = 0 \tag{3.15}$$

$$\hat{d}(K) = \hat{\beta}_{3,N+1}K^3 + \hat{\beta}_{2,N+1}K^2 + \hat{\beta}_{1,N+1}K + \hat{\beta}_{0,N+1} = d(k) \tag{3.16}$$

$$\left(\hat{\beta}_{3,n} - \hat{\beta}_{3,n+1}\right)\xi_n^3 + \left(\hat{\beta}_{2,n} - \hat{\beta}_{2,n+1}\right)\xi_n^2 + \left(\hat{\beta}_{1,n} - \hat{\beta}_{1,n+1}\right)\xi_n + \left(\hat{\beta}_{0,n} - \hat{\beta}_{0,n+1}\right) = 0 \quad \forall n = 1,\ldots,N \tag{3.17}$$

$$3\left(\hat{\beta}_{3,n} - \hat{\beta}_{3,n+1}\right)\xi_n^2 + 2\left(\hat{\beta}_{2,n} - \hat{\beta}_{2,n+1}\right)\xi_n + \left(\hat{\beta}_{1,n} - \hat{\beta}_{1,n+1}\right) = 0 \quad \forall n = 1,\ldots,N \tag{3.18}$$

$$6\left(\hat{\beta}_{3,n} - \hat{\beta}_{3,n+1}\right)\xi_n + 2\left(\hat{\beta}_{2,n} - \hat{\beta}_{2,n+1}\right) = 0 \quad \forall n = 1,\ldots,N \tag{3.19}$$

where (3.14) enforces the behavior of the cubic spline,(3.15) and (3.16) enforce the water balance equations, (3.17) enforces the continuity constraint at each knot, and (3.18) and (3.19) enforce the smoothness of the first and second derivatives of the cubic spline at each knot [4]. Note that this constrained optimization problem is still convex and quadratic.

Here, then, we return to Figure 3-3 and Figure 3-4. The fourth row in Figure 3-3 shows the difference function fit using cubic splines. Knots were placed at 12-hour intervals (i.e., at each tick mark). (The results were not particularly sensitive to the position of the knots.) As the left plot shows, this regression tracks the underlying difference function while satisfying the water balance constraints. This results in substantially more variation in the fitted bias function, transitioning from a maximum value of approximately 200 m^3/s to a minimum value of approximately -250 m^3/s. Looking at Figure 3-4, it is clear that these changes do not significantly affect the shape of the inflow profile. However, the open-loop forebay elevation computed using the inflow estimated from the cubic spline regression does a significantly better tracking of the measured forebay elevation, rarely deviating more than a couple of centimeters from the measured forebay elevation. This is an excellent result, and it would appear as though we have met the original objectives that we set out to achieve with this state estimation algorithm: track the measured forebay elevation, maintain the water balance, and preserve the shape of the measured flow.

However, an additional problem appeared when estimating the outflow from Priest Rapids Dam, the last hydropower plant in the Mid-Columbia system. Due primarily to fish-related restrictions on turbine discharge and spill, Priest Rapids will often operate in modes where its turbine discharge profile is relatively constant (i.e., varying no more than 50 m^3/s from a particular setpoint). Figure 3-5 and Figure 3-6 show the difference functions, forebay elevations, and estimated turbine discharges for Priest Rapids Dam. The layout of the plots is identical to what was shown previously in Figure 3-3 and Figure 3-4 when estimating the inflow into Grand Coulee Dam. For each type of regression, we used the same procedure for all seven hydropower plants in the Mid-Columbia. So, for the first row of plots, the inflow into the Priest Rapids forebay was the measured outflow from Wanapum Dam upstream. Likewise, in the second row of plots, the inflow into the Priest Rapids forebay was the estimated outflow from Wanapum Dam, which was estimated using the linear regression procedure described in (3.9), and so on for the third, fourth, and fifth rows of plots. This is why the underlying difference function is slightly different for each type of regression.

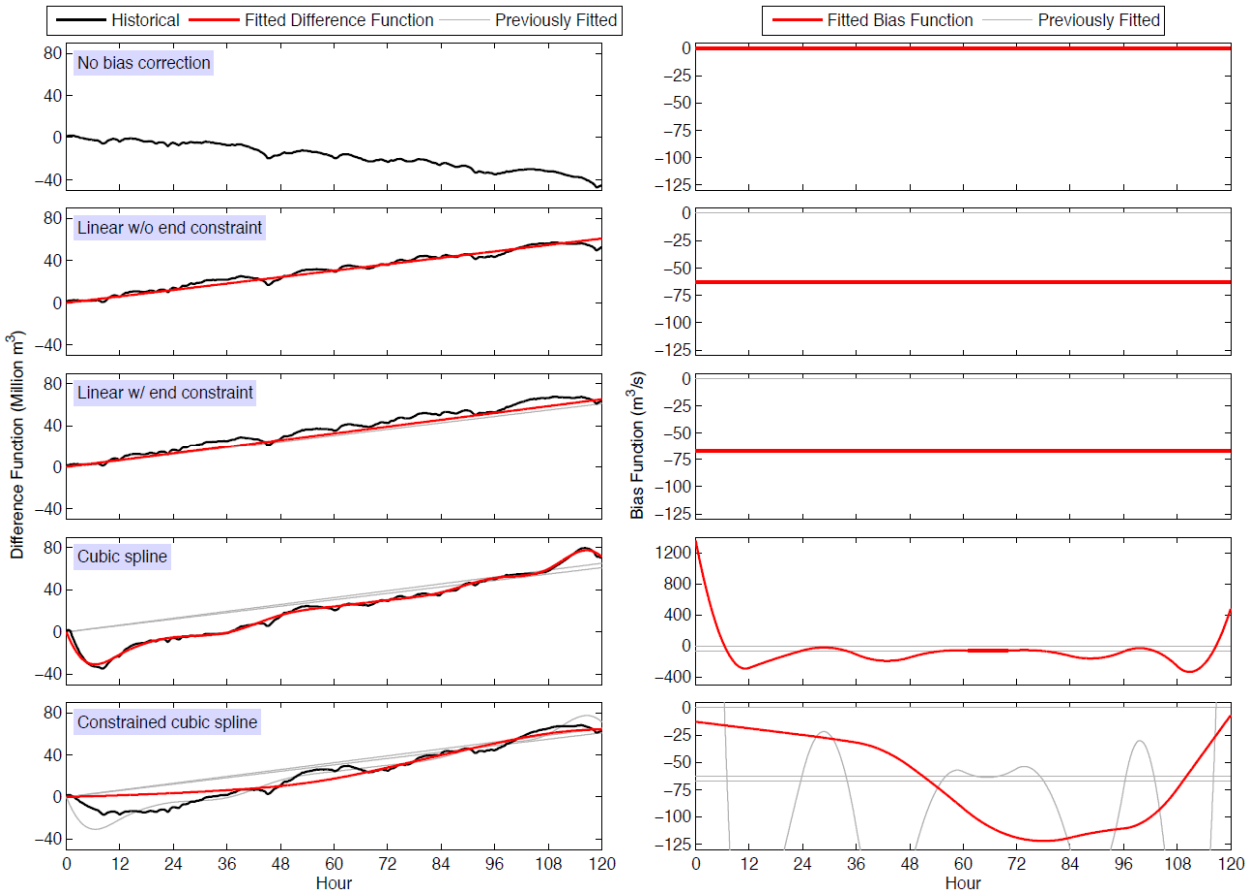

Figure 3-5
These plots pertain to the estimation of the outflow from Priest Rapids Dam. The left column of plots shows the difference function in black and the fitted difference function in red. The right column shows the derivative of the fitted difference function, which can be interpreted as the bias. In order from top to bottom, the rows show the results for no correction, linear difference function, linear difference function with water balance constraint, cubic spline, and cubic spline with ramping constraint. The knots for the cubic spline were located at each 12-hour interval (i.e., the tick marks on the x-axis).

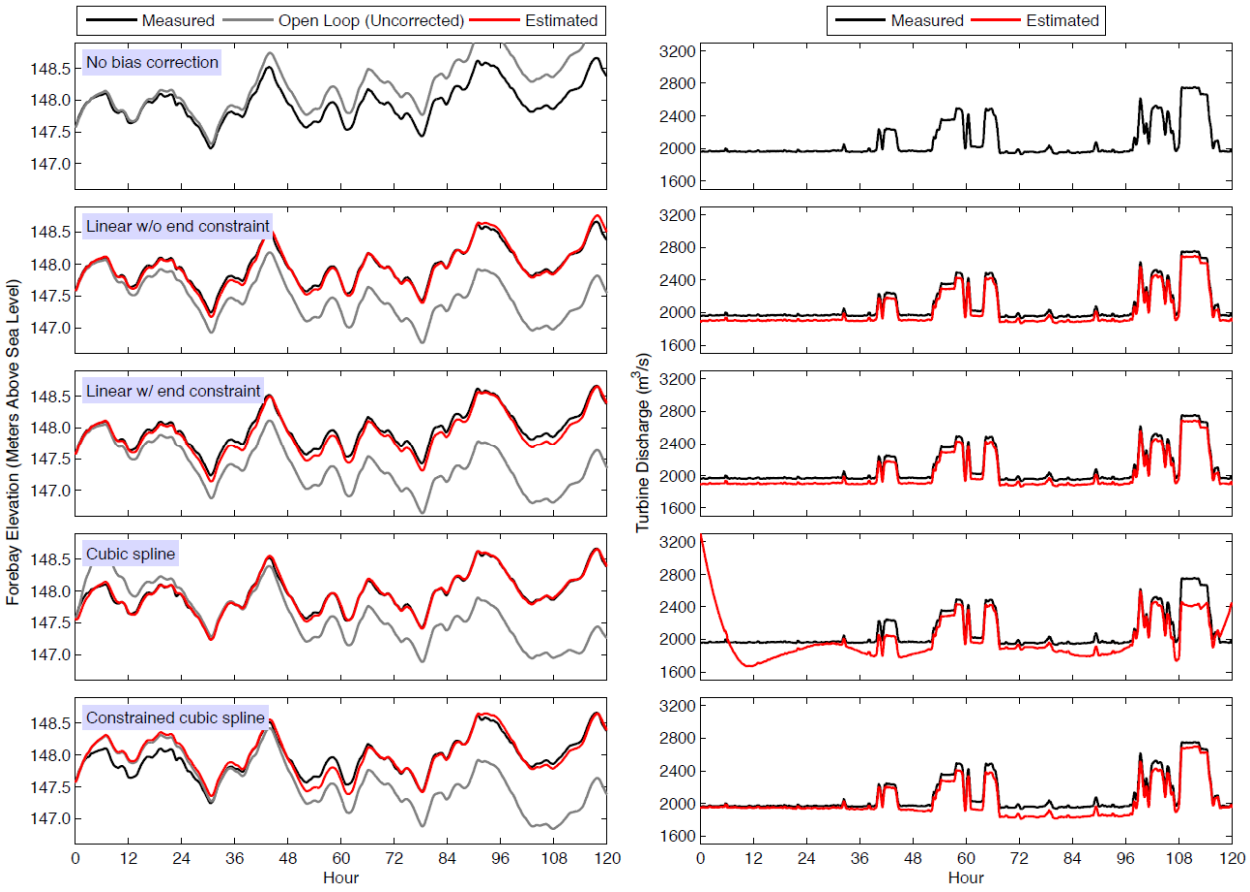

Figure 3-6
These plots pertain to the estimation of the outflow from Priest Rapids Dam. The left column of plots shows the measured forebay elevation in black, the open-loop forebay elevation using the measured outflow in grey, and the open-loop forebay elevation using the estimated outflow in red. The right column shows the measured outflow in black and the estimated outflow in red. In order from top to bottom, the rows show the results for no correction, linear difference function, linear difference function with water balance constraint, cubic spline, and cubic spline with ramping constraint.

Looking at the plots for Priest Rapids, we notice that the performance of the linear models is substantially better compared to Grand Coulee Dam. This is because the difference function is fairly linear---indicating a constant bias in the outflow measurements---and hence is well-suited to the one-parameter linear regression we discussed previously. However, the cubic spline presents some unwanted behavior. While the simulated open-loop forebay elevation tracks the measured forebay elevation with centimeter precision, the estimated outflow does not look like the measured outflow in the slightest. This is because the ramp in the bias signal at the start of the simulation period (the right plot in the fourth row of Figure 3-5 is enormous compared the fairly flat turbine discharge profile. Clearly, if we intend to analyze how, for example, environmental flow regulations on the Mid-Columbia affect the capabilities of the system, it is important that the estimated discharge profile is not wildly different from the measured discharge profile. However, it should not be necessary for a human to look at each difference function and decide whether the fitted function should be a linear function, cubic spline, or something else. Whatever regression procedure we elect to use should be adaptable to the circumstances.

Accounting for the ramping of the measured outflow

Our solution to this problem is to constrain the second derivative of the fitted cubic spline. Since the bias function is the first derivative of the estimated difference function, this is equivalent to constraining the first derivative of the bias function. This prevents the bias function from ramping excessively. This naturally leads to a follow-up question: what dictates how much ramping should be allowed? It is important that the estimated outflow mimics the profile of the measured outflow. Hence, if the measured outflow ramps substantially, the additional ramping introduced by the bias function can be fairly large because it will be swamped by the measured outflow signal. Likewise, if the measured outflow is fairly flat—as in the case of Priest Rapids Dam in this example—then the additional outflow ramping introduced by the bias function should be fairly small so as not to transform a flat measured outflow profile into a varying estimated outflow profile. Effectively, there should be an additional constraint that ensures that the estimated outflow does not look too different from the measured outflow.

We chose to introduce a constraint that is based on the travel of the measured outflow. Signal travel is the sum of the absolute change of the value of the signal over a certain period of time. A completely flat signal will thus have zero travel and the amount of signal travel will increase as ramping increases. In order to remove the effect that high frequency variability will have on the total signal travel, we apply a moving average filter to smooth the measured outflow signal. Mathematically,

$$q^{\text{smooth}}(k) = \frac{1}{\bar{k} - \underline{k}} \sum_{k=\underline{k}}^{\bar{k}} q(k) \tag{3.20}$$

where $\bar{k} = \min\left(K, k+30\right)$ and $\underline{k} = \max\left(1, k-30\right)$. These limits correspond to a moving average window of one hour, since our data has 1-minute time resolution. The size of the moving average window and the type of lowpass filter used can change depending on the needs of the particular application.

Next, we can implement a ramping score, which measures the average absolute change in the smoothed measured outflow signal. Mathematically, this can be represented by

$$s(a,b) = \frac{1}{b-a} \sum_{k=a}^{b-1} \left| q^{\text{smooth}}(k+1) - q^{\text{smooth}}(k) \right| \tag{3.21}$$

where a and b are integers and $b > a$. Then, using this ramping score, the second derivative of the difference function (i.e., the first derivative of the bias function) can be constrained using

$$\left| 6\hat{\beta}_{3,n}\xi_{n-1} + 2\hat{\beta}_{2,n} \right| \le \tau \cdot s(\xi_{n-1}, \xi_n) \quad \forall n = 1, \ldots, N+1 \tag{3.22}$$

$$\left| 6\hat{\beta}_{3,n}\xi_{n} + 2\hat{\beta}_{2,n} \right| \le \tau \cdot s(\xi_{n-1}, \xi_n) \quad \forall n = 1, \ldots, N+1 \tag{3.23}$$

where τ is a user-defined tolerance value. This set of constraints would be added to those in (3.14) to (3.19). A smaller value of τ implies that the second derivative of the difference function will be more constrained. If τ is zero, then this is identical to the linear regression formulated in (3.10) and (3.11), and (3.12) to (3.19). Note that the qualitative interpretation of (3.22) and (3.23)

is that the value of the second derivative at each knot location (along with the endpoints) is less than the ramping score for the adjacent regions. This allows the constraint to adapt to multiple ramping modes in the simulation period (e.g., if the measured outflow is flat for some period of time and then variable for some period of time).

The improvement obtained by adding the constraints (3.22) and (3.23) can be judged by looking at the results for Priest Rapids Dam, shown in the fifth row of Figure 3-5 and Figure 3-6. The open-loop forebay elevation computed using the estimated outflow tracks the measured forebay elevation closely. Additionally, the profile of the estimated outflow is similar to the measured outflow. The first derivative of the bias function is close to zero in the part of the simulation where the measured outflow is flat (from Hour 0 to Hour 48, approximately), indicating constraints (3.22) and (3.23) are functioning as intended. In the region where the measured outflow is more variable, the bias function has the freedom to move freely and more accurately track the true difference function.

Overview and Results

In the previous section, we presented results for Grand Coulee Dam and Priest Rapids Dam in order to walk through the logical steps we took to arrive at our final state estimation algorithm. This section presents results for the rest of the Mid-Columbia system. Data was taken for the same five-day period in March 2013. Forebay elevation was available with 5-minute time resolution for each facility. Turbine discharge and spill was available with 1-minute time resolution. Natural inflow was taken from USGS gauges on the relevant tributary streams of the Mid-Columbia system [3]. Data was upsampled using linear interpolation to obtain forebay elevation and natural inflow measurements with 1-minute time resolution. Knots for the cubic spline interpolation were placed every 12 hours, such that $\xi_1 = 720$, $\xi_2 = 1440$, and so on. The tolerance was chosen to be $\tau = 10^{-4}$ using the formulation in (3.21), (3.22), and (3.23).

1. Assume the turbine discharge and spill from Grand Coulee Dam are known. Use the objective function (3.13) and constraints (3.14) to (3.19) and (3.22) to (3.23) to estimate the inflow into the Grand Coulee forebay.

2. Assume the turbine discharge and spill from Grand Coulee, the natural inflow into the Chief Joseph forebay, and the spill from Chief Joseph Dam are known. Then, estimate the turbine discharge from Chief Joseph Dam.

3. Assume the estimated turbine discharge and measured spill from Chief Joseph Dam, the natural inflow into the Wells forebay, and the spill from Wells Dam are known. Then, estimate the turbine discharge from Wells Dam.

4. Assume the estimated turbine discharge and measured spill from Wells Dam, the natural inflow into the Rocky Reach forebay, and the spill from Rocky Reach Dam are known. Then, estimate the turbine discharge from Rocky Reach Dam.

5. Assume the estimated turbine discharge and measured spill from Rocky Reach Dam, the natural inflow into the Rock Island forebay, and the spill from Rock Island Dam are known. Then, estimate the turbine discharge from Rock Island Dam.

6. Assume the estimated turbine discharge and measured spill from Rock Island Dam, the natural inflow into the Wanapum forebay, and the spill from Rock Island Dam are known. Then, estimate the turbine discharge from Wanapum Dam.
7. Assume the estimated turbine discharge and measured spill from Wanapum Dam, the natural inflow into the Priest Rapids forebay, and the spill from Priest Rapids Dam are known. Then, estimate the turbine discharge from Priest Rapids Dam.

Hence, we are estimating seven unknown quantities: the inflow into the Grand Coulee forebay and the turbine discharge from the six downstream dams. The size of each optimization problem is 40 variables and 49 constraints. Each optimization problem is solved using the interior point solver `knitro` and took approximately 10 milliseconds to solve. Solving the optimization problem portion of this state estimation procedure is not computationally intensive, especially when compared to an equivalent least-squares procedure that would have tens of thousands of variables and constraints. Such a problem would have serious computational requirements, both from a computing power perspective (i.e., the time it takes to solve such a large problem to an optimal solution) and from a numerical perspective (i.e., writing or using a solver that can reliably find the true optimal solution of such a large and highly constrained problem).

The results of this state estimation procedure for the entire Mid-Columbia system are shown in Figure 3-7 (difference function), Figure 3-8 (forebay elevation), and Figure 3-9 (estimated inflow or outflow). Qualitatively, the cubic spline interpolation tracks the underlying dynamics of the difference function closely. This manifests itself in how well the open-loop forebay elevations simulated using the estimated inflow or outflow track the measured forebay elevation. In most cases, the simulated forebay elevation does not deviate more than a few centimeters from the measured forebay elevation. And, as can be seen from looking at the plots of estimated and measured inflow and outflow, the estimated flows look virtually identical to the measured flows.

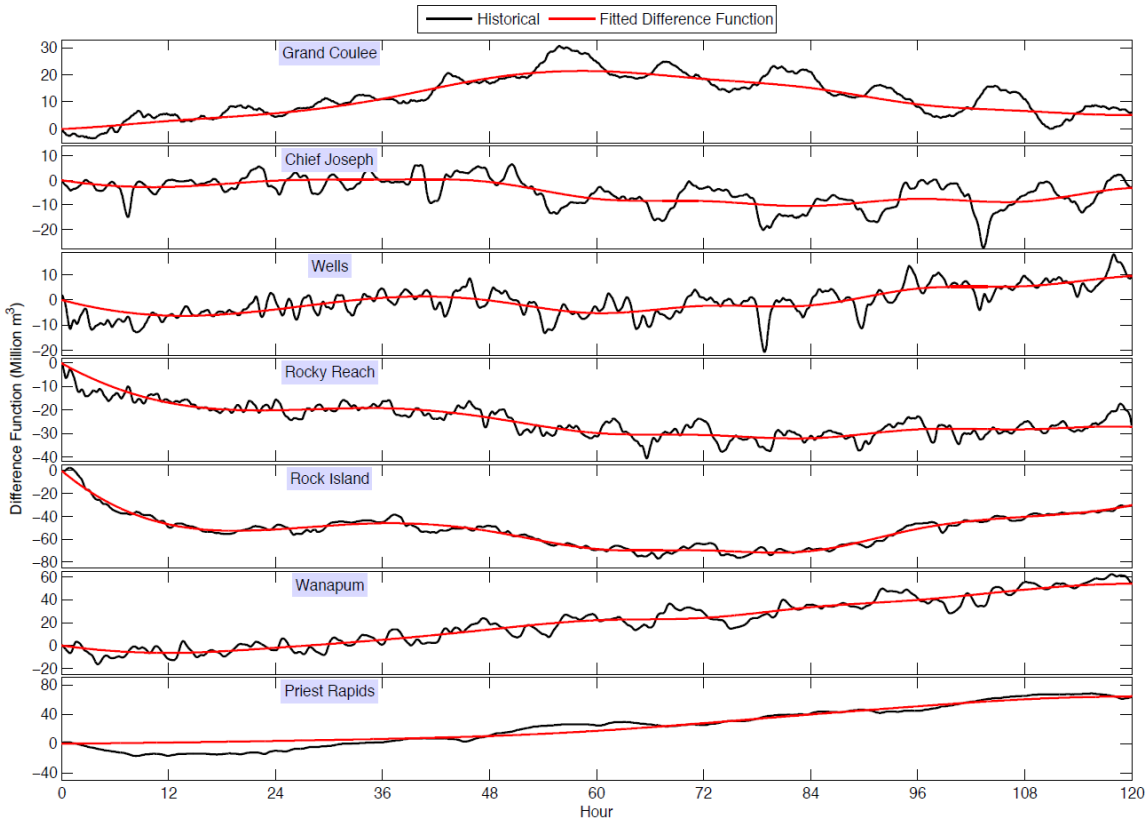

Figure 3-7
These plots shows the difference function in black and the fitted difference function in red using the constrained cubic spline estimation procedure for each of the seven estimated quantities.

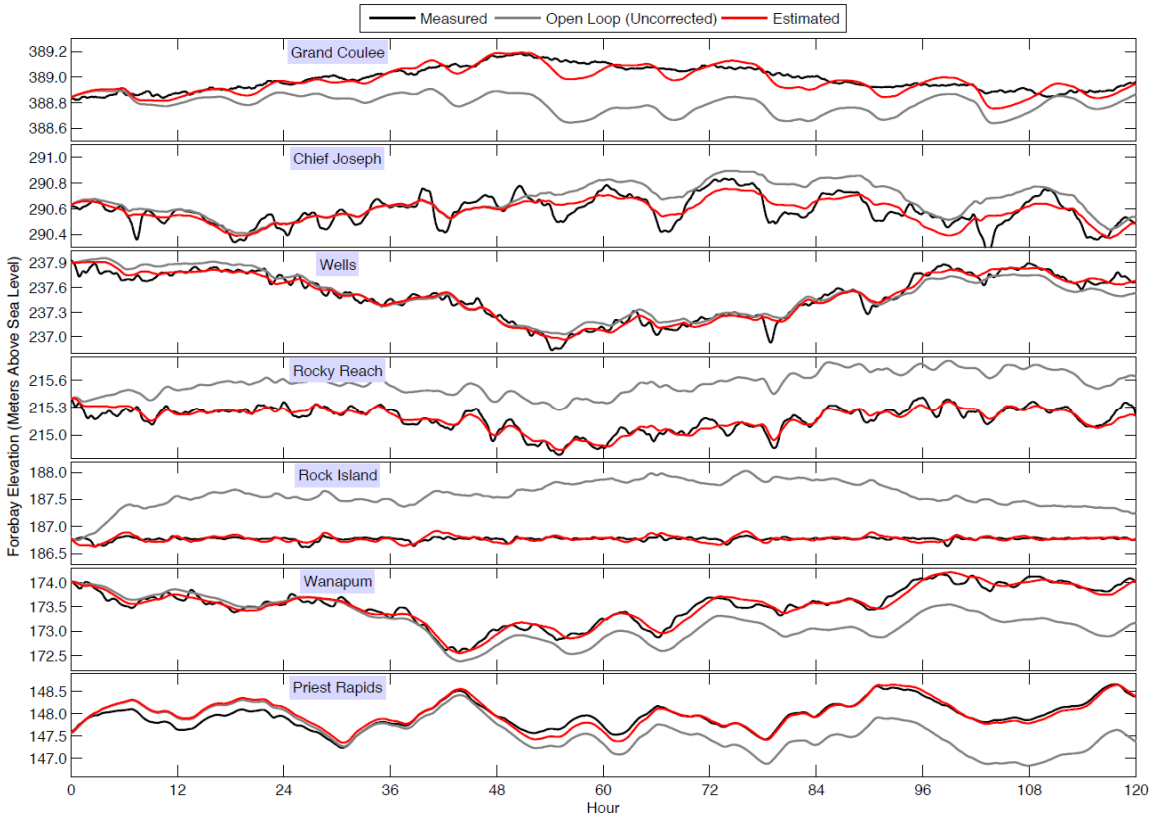

Figure 3-8
These plots show the measured forebay elevation in black, the open-loop forebay elevation using the measured flow in grey, and the open-loop forebay elevation using the estimated flow in red for each of the seven estimated quantities.

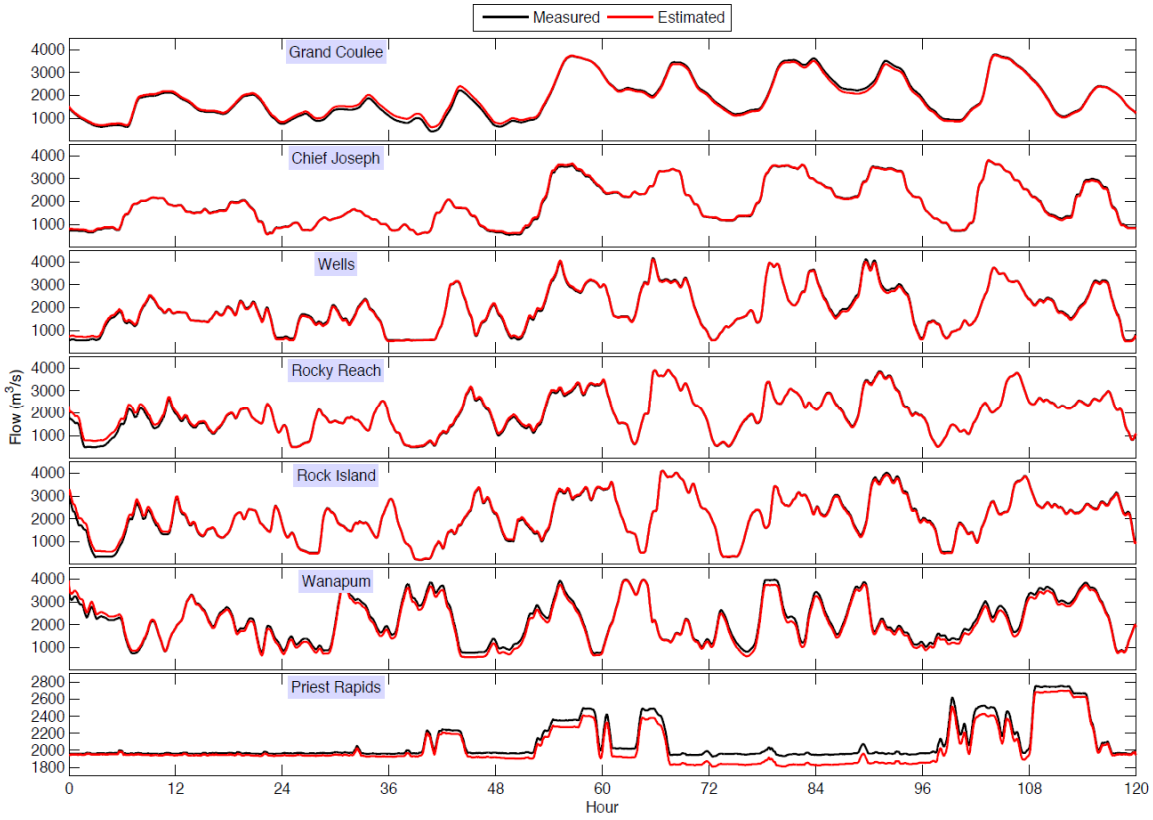

Figure 3-9
These plots show the measured flow in black and the estimated flow in red for each of the seven estimated flows.

Conclusion

This section presented an algorithm for estimating the flows in a hydropower system such that an open-loop simulation of the system using those estimated flows will yield (approximately) the measured forebay elevations. The flows are the primary control variables and the forebay elevations are the primary state variables of any hydropower system model. They capture the dynamic movement of water through the system and the static location of water in the system. The most difficult part of doing state estimation for a hydropower cascade is accounting for the tight temporal and spatial coupling of forebay elevation and flow. The goal of our procedure was to estimate these values using a heuristic algorithm where previously well-known methods had failed: least-squares because the problem was both too large and too poorly defined, and Kalman filtering because the flow measurements were biased. Our algorithm achieves the stated objectives quickly and accurately. While we make no claims about the statistical optimality of this estimation procedure, its flexibility and practical accuracy should suffice for applications in which open-loop simulations are necessary. We have implemented this state estimation procedure as an integral component of our own research on the optimal coordinated control of cascaded hydropower systems (specifically the Mid-Columbia), and it has proven to be effective. Additional steps can be taken to estimate other values of interest, including the tailrace elevation and power production from each hydropower plant, but the complexity of estimating those values is significantly reduced because the temporal and spatial coupling is minimal or non-existant.

References

1. C.-T. Chen, *Linear System Theory and Design*. 4th ed. Oxford University Press, New York, New York 2012.

2. F. Lewis, L. Xie, D. Popa, *Optimal and Robust Estimation*. 2nd ed. CRC Press, Boca Raton, Florida 2008.

3. United States Geological Survey. USGS current water data for USA. [Online]. Available: http://waterdata.usgs.gov/usa/nwis/rt

4. S. Weisberg. *Applied Linear Regression*. 3rd ed. Wiley-Interscience, Hoboken, New Jersey 2005.